The Meteorological Magazine

May 1993

SST measurements by ATSR
Stratus forecasting
Design rainfall profiles for upland areas
World weather news — February 1993

HMSO

Met.O.1010 Vol. 122 No. 1450

First published 1993

HMSO publications are available from:

HMSO Publications Centre
(Mail, fax and telephone orders only)
PO Box 276, London, SW8 5DT
Telephone orders 071-873 9090
General enquiries 071-873 0011
(queuing system in operation for both numbers)
Fax orders 071-873 8200

HMSO Bookshops
49 High Holborn, London, WC1V 6HB
(counter service only)
071-873 0011 Fax 071-873 8200
258 Broad Street, Birmingham, B1 2HE
021-643 3740 Fax 021-643 6510
Southey House, 33 Wine Street, Bristol, BS1 2BQ
0272 264306 Fax 0272 294515
9-21 Princess Street, Manchester, M60 8AS
061-834 7201 Fax 061-833 0634
16 Arthur Street, Belfast, BT1 4GD
0232 238451 Fax 0232 235401
71 Lothian Road, Edinburgh EH3 9AZ
031-228 4181 Fax 031-229 2734

HMSO's Accredited Agents
(see Yellow Pages)

and through good booksellers

£3.40 net, Annual Subscription £38, including postage.

3 8078 0010 2465 4

The Meteorological Magazine

May 1993
Vol. 122 No. 1450

551.526.6:551.507.362.2

Sea-surface temperature measurements by the ATSR

R.W. Saunders and A.H. Smith
Meteorological Office, Farnborough
D.L. Harrison
Meteorological Office, Bracknell

Summary

The Along Track Scanning Radiometer has been producing global sea-surface-temperature values since September 1991. The UK Meteorological Office has been assessing these by comparing them with their operational analysis and by carrying out a dedicated aircraft validation experiment. The initial results show an improvement in the sea surface temperature values obtained when the dual-view retrieval is used rather than a conventional nadir-only multichannel retrieval. The radiative effect of volcanic aerosols at 11 μm and 12 μm was also measured by the C-130 aircraft and found to be small but not negligible.

1. Introduction

The Along Track Scanning Radiometer (ATSR) was launched into a sun-synchronous orbit on the European Remote Sensing Satellite, ERS-1, on 17 July 1991. The primary objective of the ATSR is to measure sea-surface temperatures (SSTs) globally to an accuracy of better than 0.3 K (Barton *et al.* 1989) which is a significant improvement on previous satellite SST products (e.g. Meteosat, AVHRR/MCSST). There are several features of the ATSR described below which make this improvement possible.

This paper gives a brief description of the ATSR and outlines the results from two very different and complimentary assessments of the ATSR SST product, carried out by the UK Meteorological Office (UKMO). The first compares the ATSR near-real-time (NRT) product, which is averaged over 0.5° × 0.5° and gives good coverage between 55° S and 55° N over the earth's oceans, with the UKMO conventional SST analysis. The second assessment was a dedicated validation experiment in which the C-130 aircraft of the Meteorological Research Flight made infrared radiance measurements coincident with ERS-1 overpasses over the tropical Atlantic Ocean.

2. The Along Track Scanning Radiometer

The ATSR is a radiometer with a conical scan, inclined at an angle, so that a nadir view and forward view at a nadir angle of 47° (which translates into a zenith angle of 55.5° on the earth's surface) is obtained for each revolution of the scanning mirror. It also views two black-body targets for calibration of the infrared channels. A schematic drawing of the instrument is shown in Fig. 1 which also shows the microwave radiometer on the side of the instrument which measures total column water vapour amount. The ATSR has four channels, one at near infrared wavelengths (1.6 μm) for daytime cloud clearing, and three at thermal infrared wavelengths (3.7, 11 and 12 μm) for sea-surface temperature retrievals and cloud clearing. The field of view of the radiometer gives a 1 km pixel size at nadir on the earth's surface and the width of the ATSR swath is 500 km.

The particular features of this radiometer, which enable it to make improved retrievals of sea-surface temperatures over previous satellite radiometers, are:

(a) the combination of two views, through different path lengths of the atmosphere, allow a more accurate

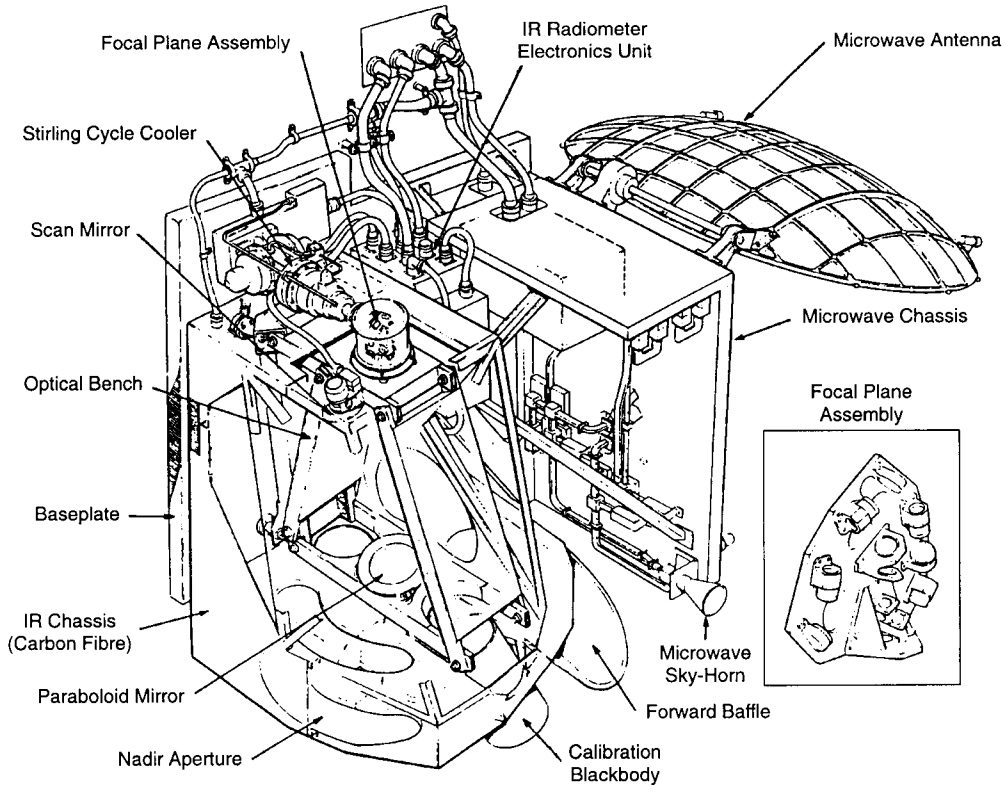

Figure 1. A schematic diagram of the Along Track Scanning Radiometer (including the microwave water vapour sounder).

correction for the intervening atmospheric absorption/emission to be made,
(b) careful design of the two calibration targets, which operate at 263 K and 303 K to encompass the full range of SSTs that are ever likely to be measured, ensure an accurate absolute calibration (< 0.1 K) can be made, and
(c) lower system noise temperatures (< 0.05 K) than achieved on other imaging infrared radiometers.

The ATSR was designed and built by a consortium of UK groups, including British Aerospace, Rutherford Appleton Laboratory, Mullard Space Science Laboratory, and the UKMO. The assembled instrument was tested in a purpose-built vacuum chamber, at the Department of Atmospheric, Oceanic and Planetary Physics, University of Oxford, to verify, among other things, the accuracy of the calibration. A more detailed description of the instrument is given by Edwards *et al.* (1990) and on the calibration by Mason (1991).

An example of an ATSR 3.7 μm brightness-temperature image over the Gulf Stream is shown in Fig. 2. The high spatial and radiometric resolution of ATSR is clearly evident in this image which shows the detailed structure of the boundaries between the hot and cold water.

Since the launch of ERS-1 the instrument had performed without any problems until 27 May 1992 when the 3.7 μm channel suddenly stopped producing data. The reason for this failure is still being investigated. The main impact of the loss of this channel is a reduced ability to detect low cloud at night.

The SST can be obtained from the measured ATSR top-of-atmosphere brightness temperatures in several different ways. During the daytime the 11 μm and 12 μm nadir brightness temperatures can be combined according to:

$$SST = \alpha T_{11} + \beta T_{12} + \gamma. \qquad (1)$$

This is the conventional 'split window' equation which has been used for many years for AVHRR SST retrievals. As β is negative, it is effectively the difference between the 11 μm and 12 μm brightness temperatures which is used to give a measure of how much infrared radiation is absorbed by the atmosphere.

In order to obtain a better correction for the atmosphere ATSR takes two measurements of the sea surface 2.5 minutes apart. The forward view at 55° to local zenith has almost twice the path length through the atmosphere compared with the nadir view. Thus a combination of the two views should give a better estimate of the effects due to the intervening atmosphere. By expanding equation (1) the dual-view retrieved SST is computed according to:

$$SST = \alpha_N T_{11N} + \alpha_F T_{11F} + \beta_N T_{12N} + \beta_F T_{12F} + \gamma \qquad (2)$$

where N and F denote nadir and forward views. The coefficients used in equations (1) and (2) have been

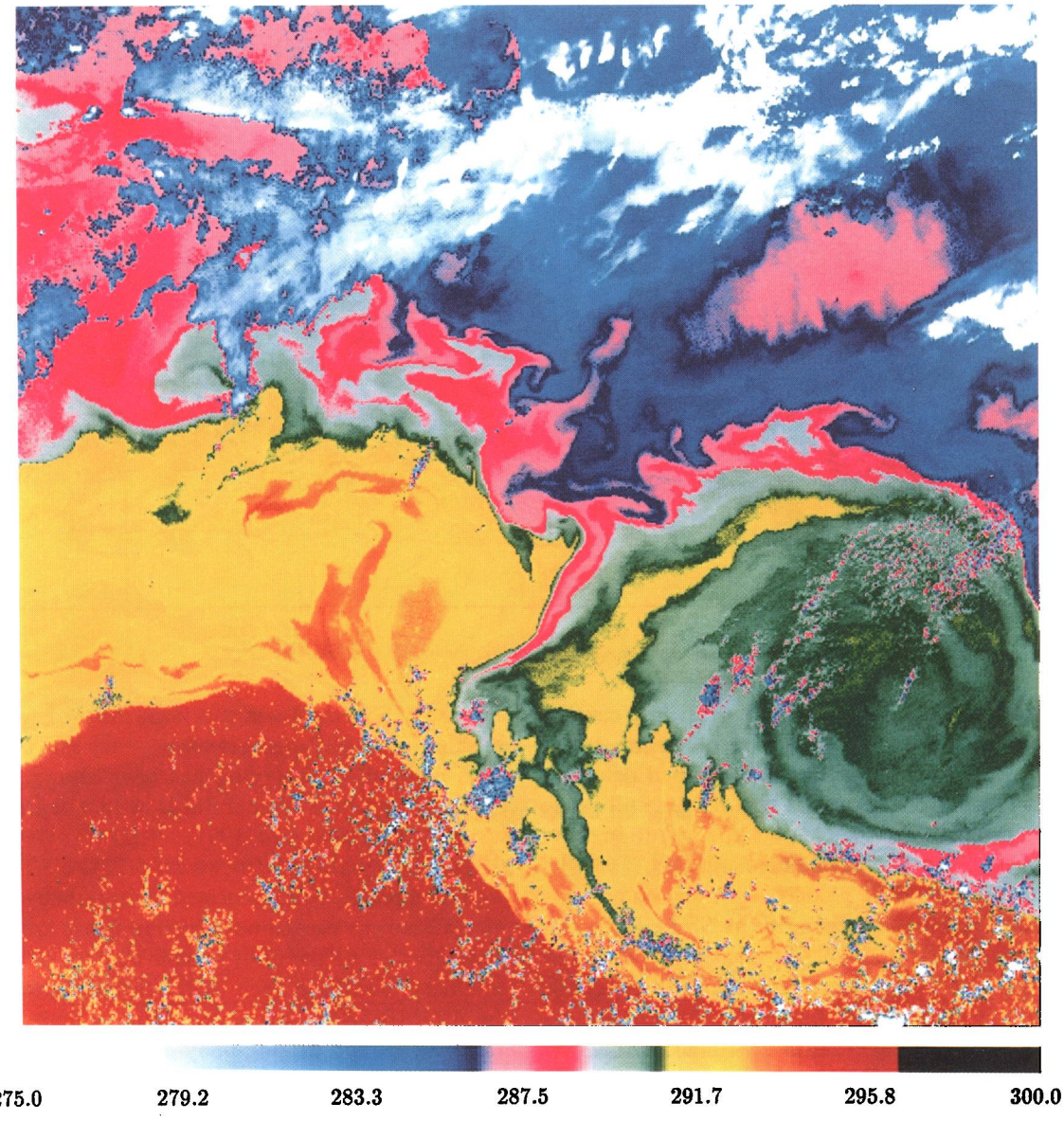

Figure 2. An ATSR nadir view 3.7 μm brightness temperature image (K) of the Gulf Stream and a warm core ring (Courtesy of Rutherford Appleton Laboratory).

derived from a radiative transfer model to give the optimum performance in a given set of atmospheric conditions (e.g. mid-latitude, tropical, polar). The coefficients also vary with across-track position. For a comprehensive review of empirical and theoretical algorithms used to retrieve SST from infrared radiometers see Barton (1992).

3. Assessment of ATSR near-real-time SSTs

The ATSR near-real-time (NRT) demonstration project was established in order to address the needs of Meteorological centres for fast-delivery (FD) data. It is a joint venture between Rutherford Appleton Laboratory, Tromsø Satellite Station and the UKMO, who is the pilot user of the data. The aim of the project is to show that the data processing and transmission system devised can provide data, of high quality and in near-real-time, to an end user. If this can be achieved then it is hoped that the system will eventually be adopted by ESA as part of the ERS-1 FD service, which currently includes products from the scatterometer and radar altimeter.

NRT products from the ATSR have been received by the UKMO since November 1991. The raw data are processed at Tromsø Satellite Station to form 0.5° × 0.5° average sea-surface temperatures (ASSTs) and the products are quality assured using data from the satellite's engineering reports. The quality-assured products are then transmitted to the UKMO within 24 hours of acquisition. On average, approximately 14 000 ASSTs are received per day. Reasonable coverage for latitudes between 55° N and 55° S is generated in around 10 days, as indicated by Fig. 3. At present, only sparse quantities of data are obtained for higher latitudes. This is due to

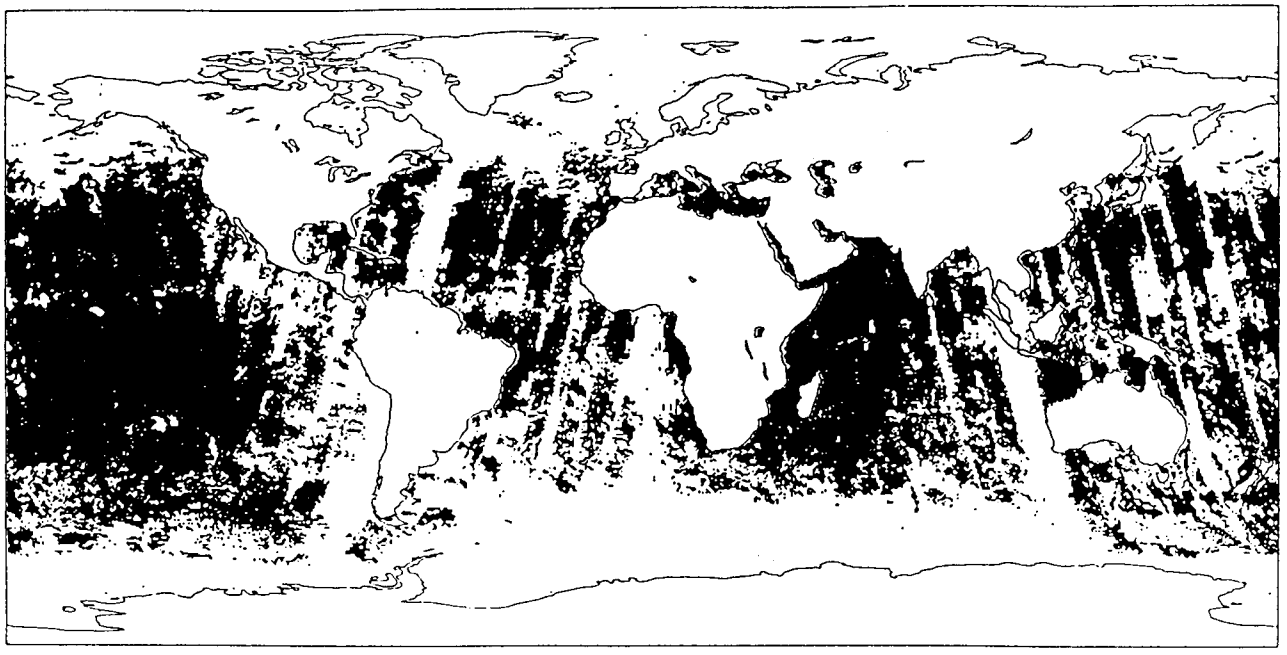

Figure 3. Distribution of ATSR ASSTs for the period 1–10 September 1992.

imperfections in the cloud screening procedure causing an overestimation of the number of measurements contaminated by cloud. Optimization of the cloud detection thresholds has proved a complex task, and is still going on. Future modifications should go some way to improving the coverage obtained at mid/high latitudes.

The quality of the NRT products are assessed primarily by comparison with coincident SSTs from the UKMO's operational analysis. The analysis is performed once per day and incorporates observations from surface marine sources (i.e. ships, buoys and bathythermospheres) received, via the GTS, in a 24-hour period. The observations undergo quality control and then a background field, simply the previous analysis, is updated by incorporating the new observations using an iterative assimilation scheme. A detailed description of the operational SST analysis scheme is given by Jones (1991). The comparison of this *in situ* analysis and the NRT product has been useful in several respects. During the initial period of ATSR operation, anomalies in the NRT processing system were rapidly identified and corrected, and the impact of subsequent changes to the data processing system could be easily evaluated.

A global mean bias of approximately −1 K with respect to the SST analysis has been persistent throughout the lifetime of the project. Part of this negative bias can be attributed to the genuine difference between the radiative skin temperature of the oceans, as measured by the ATSR, and the sub-surface bulk temperature measurements from ships and buoys. This is generally of the order of several tenths of a degree Kelvin, but varies with a number of factors including surface wind stress, solar insolation and cloud cover (Schluessel *et al.* 1990). Other factors which may contribute to the detected bias are diurnal effects and the incomplete screening of cloud. The use of SST measurements made via the engine intake of ships in the SST analysis scheme may also be a factor. This method of observing has been shown, in many cases, to produce temperatures with a warm bias of around 0.3 K (Kent *et al.* 1991).

An additional study in which ATSR NRT products were compared with collocated drifting buoy measurements has been carried out. Drifting buoys are generally considered to be the most reliable sources of SST measurements and have been used extensively to calibrate the AVHRR SSTs. Spatial and temporal limits for collocated ATSR and drifting-buoy observations were set at 0.5° latitude/longitude and ±3 hours. Fig. 4 shows ATSR drifting-buoy temperatures plotted for day and night-time observations made during July 1992. The day-time data show an overall bias of −0.5 K: but the night-time bias increases to −0.8 K. The daytime results are very encouraging as the remaining bias can largely be explained by the skin-bulk temperature difference. The poorer performance of night time ASSTs is the result of the loss of the 3.7 μm channel and the consequent problems in identifying low-level cloud at night. These results further highlight the limitations of ship SSTs and their impact on the quality of the operational analysis.

The difference between ASSTs calculated from single-view data and those derived from dual-view data has been examined. ASSTs based on single-view data are returned where only one view is cloud-free. Table I shows the bias with respect to the bulk analysis for both single- and dual-view data and demonstrates the increased agreement attainable using the dual-view algorithm. This is not surprising: the single-view algorithm is intrinsically less successful in correcting for atmospheric attenuation and the single views tend to originate from more cloudy areas and are hence more prone to error

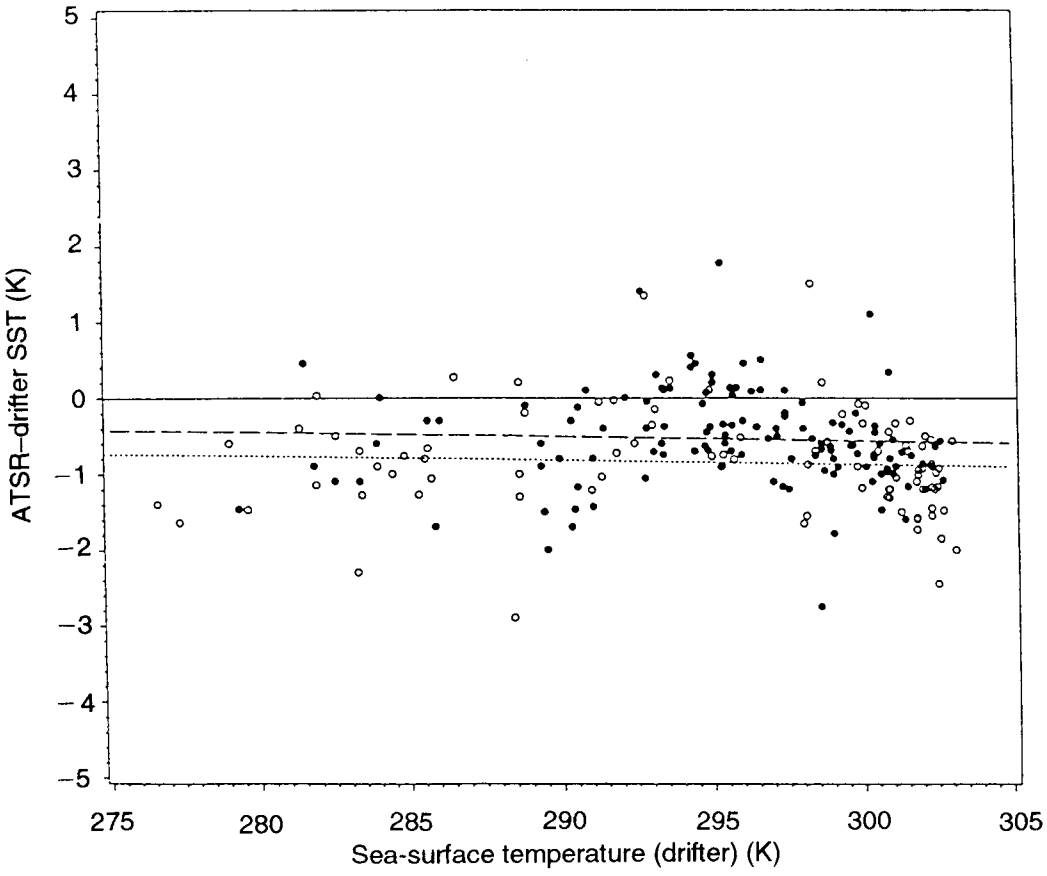

Figure 4. Collocated ATSR and drifting buoy observations for July 1992 for day (solid circles, dashed line) and night (open circles, dotted line).

Table I. Bias with respect to the SST analysis of ATSR single- and dual-view data for September 1992. O is observation, A is analysis and C is climatology.

Latitude	No. of ASSTs		Mean O–A		Stnd Dev O–A		Dual-single
	Single	Dual	Single	Dual	Single	Dual	
60–90°N	186	N/A	−1.70	N/A	0.88	N/A	N/A
30–60°N	15150	12176	−1.07	−1.06	0.74	0.80	0.23
0–30°N	25078	61389	−1.85	−1.13	0.65	0.62	0.46
0–30°S	28779	82544	−1.53	−1.00	0.55	0.56	0.38
30–60°S	32826	25452	−1.66	−1.35	0.75	0.80	0.30
60–90°S	1996	44	−1.57	−1.87	0.61	0.51	0.04
All	109703	15	−1.58	−1.10	0.67	0.63	0.38

(Lorenc *et al.* 1992). Further evidence of the increase in performance possible using the dual-view technique is obtained by looking at the difference between dual-view ASST and the corresponding ASST derived from the nadir view only. The differences are plotted in Fig. 5. The areas where the largest discrepancies occur are concentrated around the tropics which coincides with the location of the greatest concentration of water vapour and hence largest atmospheric correction. Although the improved performance demonstrated by the dual-view technique is very encouraging, the results are by no means conclusive: the improved performance may simply be a reflection of errors in the single-view retrieval algorithm.

One reason for the evaluation of ATSR NRT data is to deduce whether the data are of sufficient quality to be used in the UKMO operational SST analysis scheme. Other sources of satellite data have been used in the past: AVHRR and Meteosat data were used until shortly after the eruption of Mount Pinatubo in June 1991, when it became evident that aerosols forced into the stratosphere as a result of the eruption were having a detrimental effect on the quality of the SST retrievals (Reynolds 1991). The dual-view technique of the ATSR should mean that accurate SST retrievals are possible even under conditions of high aerosol concentrations. Validation statistics for dual-view ATSR NRT data and other sources of SST data are shown in Table II. The

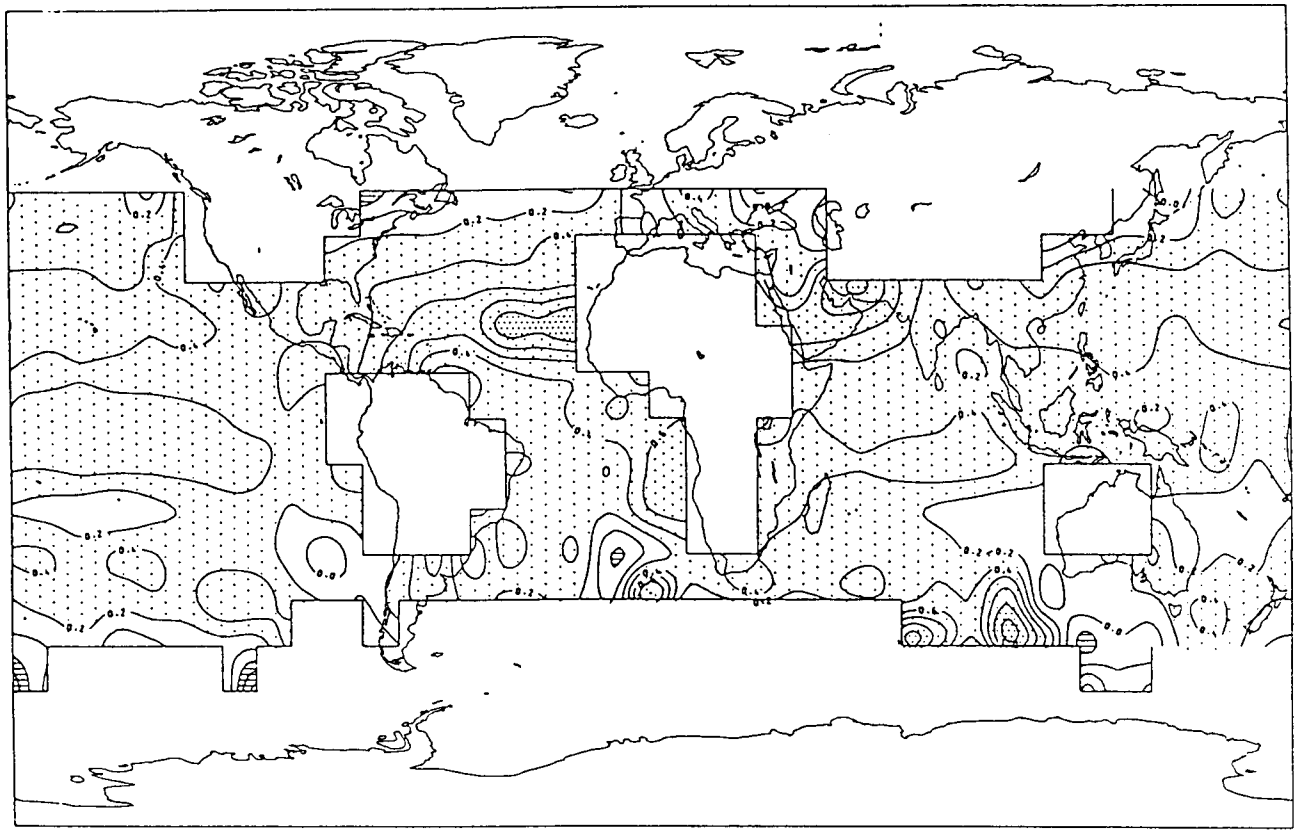

Figure 5. Global distribution of differences between dual and single-view ASSTs for September 1992 (ignore values over land).

Table II. Global statistics for all SST observation types for September 1992. O is observation, A is analysis and C is climatology.

Observation Type	N	Mean		Standard deviation	
		O–A	O–C	O–A	O–C
Ships	55127	0.06	0.24	1.05	1.17
Moored buoys	43978	−0.02	0.19	0.52	0.68
Drifting buoys	35182	−0.04	−0.09	0.36	0.56
Bathythermospheres	1186	0.18	0.44	0.41	0.53
Meteosat	30998	−0.47	−0.49	0.75	0.72
GMS	15884	−0.97	−1.90	1.12	1.16
AVHRR (NOAA-11)	90987	−0.13	−0.08	0.68	0.70
ATSR (ERS-1)	181605	−1.10	−1.01	0.63	0.65

other satellite-derived SSTs (from the NOAA polar-orbiting satellites with AVHRR and the European (Meteosat) and Japanese (GMS) geostationary platforms) are derived using algorithms that are empirically calculated against *in situ* data. They are therefore estimates of bulk SST and have smaller biases than obtained from ATSR dual-view data but comparable standard deviations. The standard deviation for ship data is considerably larger. Trial analyses using only ATSR data have been produced (Fig. 6). Differences between these and the *in situ* analysis have been investigated and show little dependence on geographical location. This illustrates the potential value of ATSR data once a suitable method for eliminating the bias between the *in situ* and radiative SSTs has been established. One short-term solution is to devise an empirical bias correction scheme based on selected high-quality surface observations. A better approach is to parameterize the skin effect using model-derived surface-wind stress and heat fluxes but this will take some time to develop.

4. The First ATSR Tropical Experiment

As part of the ATSR validation programme the UK Meteorological Office Research Flight carried out the First ATSR Tropical Experiment (FATE) in November 1991. The primary objective of FATE was to validate ATSR top-of-atmosphere radiances and retrieved SSTs in tropical atmospheres using a multichannel radiometer (MCR) (Kilsby *et al.* 1992) on the C-130 aircraft. Two of the channels on the MCR were closely matched in spec-

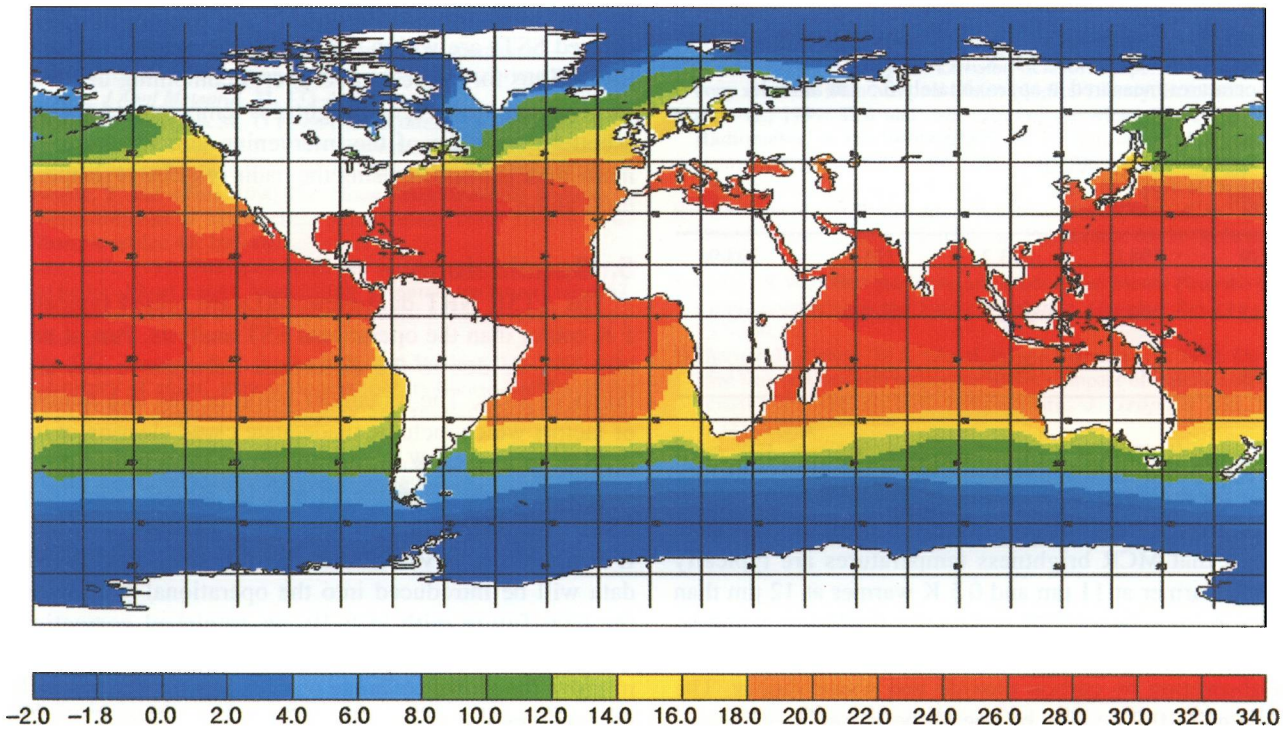

Figure 6. SST analysis (°C) from ATSR data valid for 18 August 1992. This analysis is derived initially from climatology and then replaced by ATSR data up to 10 days old.

tral response to the 11 μm and 12 μm channels of ATSR. MCR radiances were also measured at a number of levels between 70 m and 8 km altitude to provide a radiance profile which could be compared with that predicted by the Rutherford Appleton Laboratory radiative transfer model used to derive the SST retrieval coefficients for equations (1) and (2). These profile data are not presented here but in a more comprehensive paper on the FATE measurements (Smith *et al.* 1993).

Fig. 7 shows the region around Ascension Island (8° S, 14° W) where FATE was carried out. The areas flown for three clear-air flights A139, A143 and A144 (1, 7 and 8 November 1991, respectively) are shown with the ERS-1 sub-satellite track for flights A139 and A143 superimposed. During each of the three clear air flights, the MCR was recording brightness temperatures at a height of approximately 6.5 km within five minutes of an ERS-1 overpass of the area. Table III shows the averaged

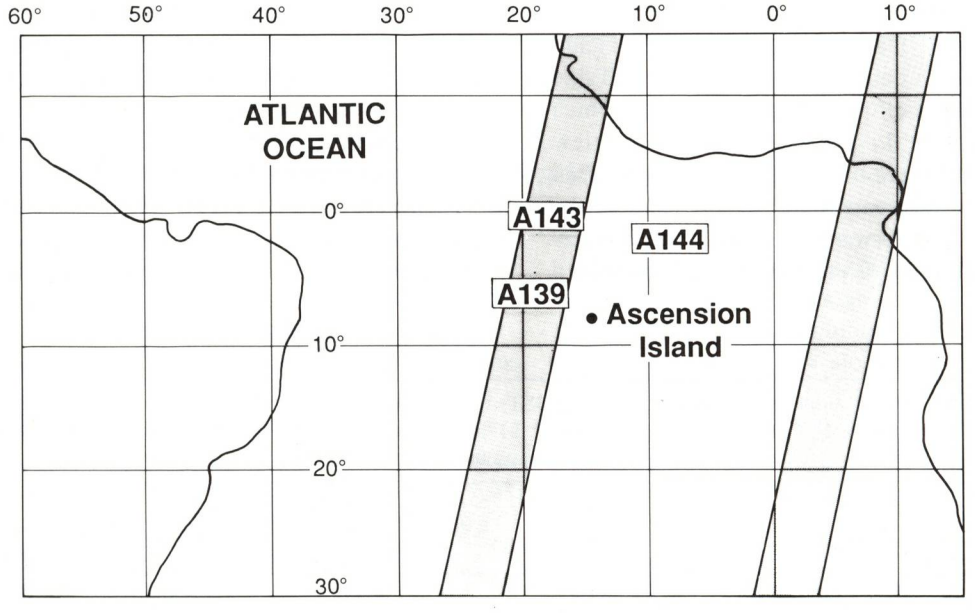

Figure 7. Locations of C-130 clear-air flights A139, A143 and A144 during FATE. The shaded area is the ATSR swath for flights A139 and A143.

Table III. Comparison of ATSR 11 μm brightness temperatures (K) with coincident MCR 11 μm and 12 μm brightness temperatures measured at approximately 6.5 km altitude.

	Nadir view			
	ATSR		MCR	
Flight	11 μm	12 μm	11 μm	12 μm
A139	294.0	293.2	295.0	293.9
A143	293.3	292.0	293.9	292.4
A144	292.0	290.8	292.7	291.3

nadir MCR and coincident ATSR brightness temperatures for the three clear-air flights. Each MCR average is taken over a run of approximately 5 minutes. The table shows that MCR brightness temperatures are typically 0.7 K warmer at 11 μm and 0.5 K warmer at 12 μm than the corresponding ATSR nadir view brightness temperatures. Half of this difference is due to residual atmospheric absorption by carbon dioxide and water vapour. The remainder (0.3 K) may be due to the presence of stratospheric aerosols at a level between the aircraft (6.5 km) and ATSR (777 km), as seen by other instruments on the C-130 (Saunders 1993).

Approximately 100 minutes after the ERS-1 overpass, the C-130 aircraft flew down to a low level above the sea surface in order to measure the radiative SST (i.e. the measured sea-surface brightness temperature corrected for reflected sky radiation) using the MCR and the PRT-4 (8–13 μm) radiometer on the C-130. Both of these radiometers have an absolute measurement accuracy of 0.3 K. The measured radiative SST was averaged over a period of approximately five minutes for a nadir view 70 m above the sea surface. The nadir and forward ATSR 11 μm and 12 μm brightness temperatures in Table III are used to estimate the SST according to equations (1) and (2). The results of both computations are given in Table IV which show that for all three flights, the SSTs which are derived using only 11 μm and 12 μm nadir view brightness temperatures are on average 2.2 K cooler than the actual radiative SST as measured at low level by the C-130. When the ATSR forward-view brightness temperatures for the 11 μm and 12 μm channels are combined with the nadir views according to equation (2) the ATSR-derived SSTs are within 0.8 K of the measured radiative SSTs. Thus for tropical atmospheres combining the nadir and forward view ATSR brightness temperatures enables a better correction of the intervening atmosphere to be made than is possible using the nadir brightness temperatures alone.

5. Conclusions

The ATSR NRT dual-view SSTs are biased typically 1 K colder than the operational SST analysis. Part of this bias will be due to the difference between *in situ* and radiative SSTs. The remainder could be due to a number of factors which include: inadequate cloud clearing of the ATSR data, biases in the retrieval algorithm due to uncertainties in the radiative transfer model and/or ship SSTs from engine intakes biasing the analysis too warm. It is likely that AVHRR and daytime dual-view ATSR data will be introduced into the operational analysis in the near future with initially an empirical correction based on *in situ* data applied. This will dramatically improve the global coverage provided by the various SST data sources.

For a tropical atmosphere, the aircraft radiometer measurements also show a cold bias of the retrieved dual view ATSR SSTs of about 0.7 K when compared with low-level aircraft radiometric SST measurements. This bias increases to greater than 2 K when only single-view retrievals are used. The effect of the volcanic aerosols from the Mount Pinatubo eruption was to reduce the nadir ATSR 11 μm and 12 μm brightness temperatures by up to 0.7 K and 0.4 K, respectively

Acknowledgements

The ATSR was funded by the UK Science and Engineering Research Council and the NRT project was funded by ESA. Thanks are due to Wing Commander Blake for allowing the UK Meteorological Research Flight C-130 to operate out of Ascension Island and the RAF aircrew for their expert flying and continual guidance in planning and executing this campaign. The Space Science Department of the Rutherford Appleton Laboratory provided the FATE ATSR data and also gave helpful advice on analysing these data. The ATSR analysis was provided by C.P. Jones (Meteorological Office).

Table IV. Comparison of ATSR retrieved SSTs and brightness temperatures (K) measured at 70 m above the sea surface by the MCR 11 μm channel and the PRT-4 radiometer (8–14 μm). Each value is an average of a 5-minute straight and level run.

Flight No.	ATSR nadir view	ATSR nadir + forward views	MCR 11 μm B temp.	PRT-4 8–14 μm B temp.
A139	296.0	297.4	298.0	298.0
A143	296.6	298.2	299.0	299.0
A144	295.0	296.6	296.9	297.3

References

Barton, I.J., 1992: Satellite-derived sea surface temperatures — A comparison between operational, theoretical and experimental algorithms. *J Appl Meteorol*, **31**, 433–442.

Barton, I.J., Zavody, A.M., O'Brien D.M., Cutten, D.R., Saunders R.W. and Llewellyn-Jones, D.T., 1989: Theoretical algorithms for satellite derived sea surface temperatures. *J Geophys Res*, **94**, 3365–3375.

Edwards, T. and others, 1990 The Along Track Scanning Radiometer Measurement of sea surface temperature from ERS-1. *J Br Interplanet Sci*, **43**, 160–180.

Jones, C.P., 1991: The operational sea surface temperature analysis scheme. Short range forecasting research technical note 67. (Unpublished, copy available from National Meteorological Library, Bracknell.)

Kent, E.C., Truscott, B.S., Taylor, P.K. and Hopkins, J.S., 1991: The accuracy of ships' meteorological observations: Results of the VSOP-NA. Marine Meteorology and related Oceanographic Activities 26, W.M.O.

Kilsby, C.G., Edwards, D.P., Saunders, R.W. and Foot, J.S., 1992: Water vapour continuum absorption in the tropics; aircraft measurements and model comparisons. *Q J R Meteorol Soc*, **118**, 715–748.

Lorenc A.C., Bell R.S., Foreman S.J., Holt M.W., Offiler D., Hall C.D., Harrison D.L. and Smith S.G., 1992: The use of ERS-1 products in operational meteorology. S Division Scientific paper. (Unpublished, copy available from National Meteorological Library, Bracknell.)

Mason, G., 1991: Test and calibration of the Along Track Scanning Radiometer, A satellite borne infrared radiometer designed to measure sea surface temperature. D.Phil. Thesis, Dept of Atmospheric, Oceanic and Planetary Physics, University of Oxford.

Reynolds, R.W. 1991: Effects of Mt. Pinatubo on NMC/CAC SSTs. World Climate Research Programme Publication, 63, J1–8. Geneva, WMO.

Saunders, R.W., 1993: Radiative properties of the Mount Pinatubo volcanic aerosols over the Tropical Atlantic. *Geophys Res Lett*, **20**, 137–140.

Schluessel, P., Emery, W.J., Grassl, H. and Mammen, T., 1990: On the bulk-skin temperature difference and it's impact on satellite remote sensing of sea surface temperature. *J Geophys Res*, **95**, 13341–13356.

Smith, A.H., Saunders, R.W. and Zavody, A.M., 1993. The validation of ATSR using aircraft radiometer data over the tropical Atlantic. (Submitted to *J Atmos Oceanic Phys*).

Editor's note. The technique below has been developed by an outstation forecaster. Purists may argue that it should be supported by tables of statistics and deep theoretical justification. Either requirement would probably suppress this work. Instead I offer it to all as it stands and will welcome comment on its efficacy. Sceptics should note that the method described below is in close accord with that suggested by W.E. Saunders (1950) at the end of his original paper on fog forecasting. It is a long time since a work of this type was printed here. I hope it will inspire others to exercise their minds and not rely entirely on output from a powerful, remote computer.

551.509.324.1

Stratus forecasting

D.V. Warne

Until recently at Meteorological Office, Wattisham

What follows is a method of forecasting stratus but is, perhaps more importantly, a new way of looking at the basic concept of instability and applying this to the forecasting of cloud (and visibilities up to a point) in the boundary layer.

When I first became a forecaster I was, I remember, very surprised to discover that on some summer evenings the relative humidity rose very quickly, to the point where I became worried as to whether we were going to get fog: in fact the visibility remained good, perhaps 15 miles. It was clear to me even at that time that there must be a limit beyond which the visibility would decrease. This limit eventually became my 'critical visibility line' — what I now call the **Critical Theta-W (CTW)**.

Having selected the most relevant ascent, I draw in the saturated adiabatic through the wet-bulb temperature from the base of the boundary layer inversion (there usually is one) down to the surface isobar and call this the CTW. Occasionally it may be necessary to use the wet-bulb at a somewhat lower level if this is significantly moister. I believe that the air beneath the boundary layer inversion continues its slow overturning as cooling progresses — note the continued twinkling of any lights — until the surface wet-bulb temperature passes below this value. On the tephigram this is when the surface wet-bulb temperature passes to the left of the CTW. This also means that the cloud which forms as a result, to the left of the line, is basically stable and of the true stratus type,

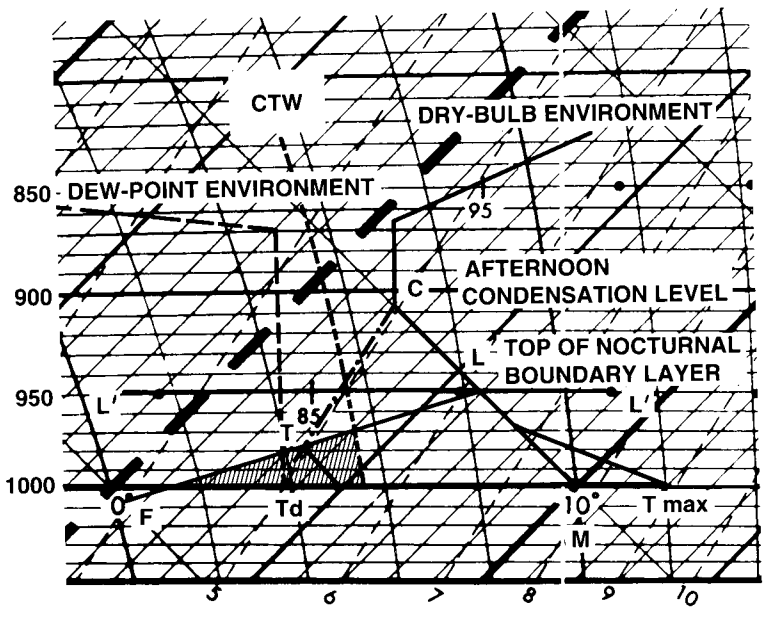

Figure 1. The stratus construction lines (on a tephigram) on an ideal sounding with a gradient wind of 30 kn. True stratus forms in the shaded area, 'cumulostratus' in the area between ML at the CTW.

whereas cloud forming to the right of the line is basically unstable and convective (although it may be at, say, 200 ft).

I regard this concept of the CTW as fundamental to the forecasting of cloud within the boundary layer. Let me give you an example of the way in which it works.

In February 1993 there was a cooling anticyclonic inversion at around 3000 ft, beneath which there was a persistent Sc sheet. The wind across the United Kingdom was south-easterly and the thickness of the Sc decreased to around 1000 ft early in the night. About this time the cooling at the inversion caused the CTW to drift to a value below the surface dew-point and Cu formed with a base of 800 ft: this supported the Sc sheet until surface cooling brought the dew-point back below the CTW and convection stopped allowing the stratocumulus to disperse.

The method for forecasting stratus (refer to Fig. 1)

(1) Construct the night cooling curve — using a proven method for your station.

(2) Find the best (usually the only!) upwind ascent and plot the lower layers on an open-scale tephigram.

(3) On the tephigram mark the θ_w line representing the **CTW** as described above.

(4) Mark on the station surface pressure line FM.

(5) On the surface pressure line mark the **fog-point**, F. The Saunders method is probably the best method in the United Kingdom.

(6) The next task is to assess the mean depth of the nocturnal mixing layer. Unless the gradient is clearly changing it is expedient to use the actual — usually mid-afternoon — value. It has proved reasonable to take the depth to be 10 hPa for every 6 kn of gradient. For example a gradient of 30 kn gives a nocturnal mixing layer some 50 hPa deep. Draw onto the tephigram the line representing the **top of the mixing layer**, L'L' (in this case — 50 hPa above the Surface Pressure Line). Note where the **top of the mixing layer** line cuts the **environment curve**, at L, and join this point to the fog-point, F from para. (5) to form the '**line**', LF. The **line** represents the top of any stratus cloud that may form. The position of the Normand point for surface temperature and dew-point represents the cloud base. Stratus forms when, during the cooling process, the Normand point passes to a level below the **line**. Note that a thickness of about 150 ft is necessary for stratus to be visible.

(7) Now, as cooling progresses the task is to monitor progress by plotting successive Normand points, noting the direction which these are taking (unfortunately these sometimes behave badly at first but they usually settle down — airstreams are not often homogeneous). When a reasonable pattern emerges and the Normand points are heading for the **line** it may be necessary to take readings (T, T_d) more frequently. Note where the Normand point curve seems likely to pass below the **line**, T: read off the corresponding surface temperature and the time for it from the cooling curve. Plotting the Normand point curve in this way does give the outstation forecaster an enormous feeling of confidence in the outcome, especially when surface humidity is high and neither fog nor stratus has been mentioned in the briefing!

General remarks

I have noticed that, during cooling, the Normand points usually lie on a curve that takes the form of an arc of a circle with its centre somewhere near where the environment dew-point curve crosses the level of the afternoon condensation level (above when the air is drying out, below when the air is moistening) passing

through the Normand point at T_{max} and the fog-point. It will be noticed that in winter the curves are very flat, indicating a preponderance of low cloud of the 'cumulostratus' type. In summer there is a larger proportion of cases where the curve is a quarter circle giving a good intercept with the **line** and a majority of cases of genuine stratus. (I remarked on the rapid increase in humidity in the early stages of cooling in the preamble.)

Let me now mention briefly the factors which will, clearly, alter the relative position of the **line.**

(a) A significant change in the gradient speed; a change of some 10 kn or so is necessary before we need to recalculate, bearing in mind that we will not be sure about the fog-point variation. With winds of over 35 kn there is very little nocturnal cooling at all, whereas a decrease to below 18 kn or so should point to the likelihood of fog rather than stratus!

(b) A significant change in the fog-point; this is difficult to forecast but, while following the Normand point plot as cooling proceeds this will be easy to see as the curve turns off towards the left or right and eventually aims at the new fog-point!

(c) A combination of increasing gradient and increasing fog-point will cause the line to gyrate and may leave the important section of the **line** in the same place!

It is useful to note that the highest stratus base seems to be related to the 10 m wind directly by the relation

N kn gives base *N* 00 ft.

A certain reluctance to forecast stratus with insufficient wind to support it seems prudent — unless the air is basically unstable, i.e. unless the Normand point is to the right of the CTW. We often see TAFs forecasting, say, 1000 ft with only 7 kn of wind: how can this be? Ignoring the vagaries of the TAF code; there are two possibilities, namely: instability — stratus forming for cumulus reasons and, of course, precipitation.

Our country being an island, it is always appropriate to have in mind the relationship between the upwind coastal dew-points and the sea temperatures, together with their Normand point and the CTW off the only upwind ascent. It is vital to realise that in autumn and winter sea temperatures are relatively high and more prone to produce low convective cloud given sufficient moisture at these levels, whereas in spring and summer the trend is for the more conventional stratus.

It should be noted that the descent of air down the lee side of nearby hills will have a significant effect which should be reflected in the forecasts.

With all this in mind, let us now look at the various types of stratus:

1. Nocturnal — formed by radiative cooling.
2. Post-mist — with rising temperatures.
3. Instability — stratus forming for cumulus reasons.
4. Precipitation.
5. Lifted fog — enough said!

1. Stratus forming by nocturnal radiation

Note the station maximum afternoon temperature and its dew-point. It does, of course, sometimes happen that one can take more appropriate temperatures off stations upwind, if so, then even better. Now draw the cooling curve and start the construction.

2. Post-mist stratus

After a fine night of cooling when temperatures have failed to reach the fog-point, with sufficient wind to support it, there may still be a danger of low cloud forming as temperatures rise. Clearly, as temperatures fall at night so do the dew-points (both might eventually reach the fog-point). This means that when the morning forecast is being prepared, say at 0500, the dew-points on the latest British Isles chart may be considerably below those that will be prevalent at, say, 0900, because as temperatures rise, due to solar heating, so will the dew-points. From the above it is clear that if the Normand point were to reach a position below the surface inversion (from an amended upwind midnight ascent), then stratus will form and at a time than can be predicted from tables of available radiation. The problem is to assess the progress of the dew-point. What to do? To calculate the likely maximum dew-point I have three suggestions:

(a) use the wet-bulb from the previous afternoon,

(b) use the actual (0500) upwind coastal dew-point, or

(c) use divine inspiration!

Plot the best one of these onto the chosen ascent (with its HMR line). Then draw on the dry adiabatics through the forecast hourly temperature values and just see whether at any stage in the rise of both temperature and dew-point it really is possible to find a Normand point in a position where stratus could form, however temporarily. Remember, sufficient wind is also required.

3. Instability stratus

As I have suggested, it usually helpful to keep a constant check on the relationship between the coastal temperatures and their relatively high dew-points and the position of their Normand point relative to the CTW on the upwind ascent. Stratus will not form easily at this natural condensation level unless there is moisture present at around the 800 to 1500 ft level. It does, however, sometimes occur (usually unexpectedly!) with onshore winds with quite normal fair-weather-cumulus-type midnight ascents, especially, though not necessarily, with freezing levels low enough to allow for light showers. I have seen quite a few situations over East Anglia with such 'cumulostratus' with bases as low as 300 ft, arriving mid-morning and dispersing, as is normal with cumulus cloud, during the evening.

With instability and moisture at low level this type will very occasionally form during the evening as cooling progresses, but will usually last no more than three hours or so before dispersing. Care should be taken when forecasting a major case of nocturnal stratus advection that

low cloud on the chart during the evening is not of this type!

I have seen a few occasions of this evening 'cumulo-stratus' cloud — characterized by its variability, both in time and space — where, as the temperatures fall, the Normand point traverses gradually to the left aiming towards the fog point and eventually crosses the CTW line, at which point the low cloud is suddenly transformed into ⅞–⅝ of the genuine, persistent variety. This means, of course, that on a particular chart these two types can be in juxtaposition.

4. Stratus in precipitation

I don't really know that I have anything useful to add about this but, here goes: I must admit to being too fond of over-forecasting low cloud in rain, mainly because I don't know how to forecast it in the first place! Of course, what we normally do is to follow developments upwind, unless upwind is out over the sea. With a good solid pre-warm-frontal rain area and stable conditions I often use the cloud bases at Boscombe Down as a good guide for forecasting stratus bases at Wattisham (with a south-easterly surface wind), and I am sure many of us do this sort of thing. I think it is useful to follow the natural condensation levels (as dew-points rise) and relate these to the CTW. I suggest that a good solid three hours or so of light rain gradually becoming moderate is very likely to produce cloud at these, often very low levels especially in southern England; further north the mountains complicate matters. However, especially if the air is basically unstable — note my definition above — this cloud is very dependent indeed on the presence of the rain and, should it stop, it will be off like a shot. So in this instance we can only be as good at forecasting the lowest stratus as we are at forecasting rain! On the other hand, reports of *drizzle* do seem to indicate moisture in the critical 800–1500 ft zone and really are a good indicator of the formation of persistent low cloud. Do watch out for showers by coalescence being reported as drizzle — especially in East Anglia!

Conclusion

I have just one more small point; such subjects as 'advection', and 'upslope motion' seem to me very much side issues in the local forecasting process. If one follows the evolution of temperatures at stations, stratus will form as and when the Normand point is in the right place no matter if the nearest upwind station has stratus or not.

Reference

Saunders, W.E., 1950: Method of forecasting the temperature of fog formation. *Meteorol Mag*, **79**, 213–219.

551.577.2:551.577.37:556.161(410)

The derivation of design rainfall profiles for upland areas of the United Kingdom

N.S. Reynard and E.J. Stewart
Institute of Hydrology, Wallingford, Oxfordshire, United Kingdom

Summary

The application of techniques for design flood estimation requires an understanding of the temporal variability of storm rainfall. Current practice relies on the definition of design storm profiles which seek to display a typical pattern of variability in rainfall intensity throughout an event. The paper evaluates methods of design profile construction for a range of durations from 1 hour to 11 days. In particular the effects of data type and data interval on the form of design profiles is examined.

The paper reviews various methods of design profile derivation for a range of durations and compares the results for both point and areal extreme rainfall events. Several data sources are utilized including daily rain-gauge data from north Wales and north-west Scotland and hourly data from the Hameldon Hill radar in north-west England. The synoptic meteorology giving rise to some notable rainfall events is investigated and the statistical characteristics and seasonal distribution of both the observed and the design rainfall profiles are examined.

1. Introduction

Most rainfall run-off methods for design flood estimation require the construction of rainfall profiles to distribute a design rainfall depth through time. It is difficult to characterize temporal patterns of rainfall because the precipitation process is highly variable. This paper addresses the problem of deriving temporal profiles for design applications in upland areas. The results outlined are taken from a wider study of the spatial and temporal variations of rainfall that affect reservoir safety in upland areas of the United Kingdom.

Current practice in the United Kingdom is to use the Flood Studies Report (FSR) method which represents the design rainfall by a symmetrical and unimodal profile (Natural Environment Research Council 1975). This technique is recommended only for durations of up to several days (FSR II.6). In Scotland a method has been developed to calculate design profiles for durations longer than those recommended in the FSR, as critical durations in some multi-reservoired catchments can be as long as 7 to 10 days. The method is based on the use of a number of profiles of observed rainfall events chosen subjectively (Stewart and Reynard 1991). This paper presents further results from the average variability method (Pilgrim *et al.* 1969) and analyses, among other things, the effects of season, duration and areal averaging on the form of the rainfall profiles.

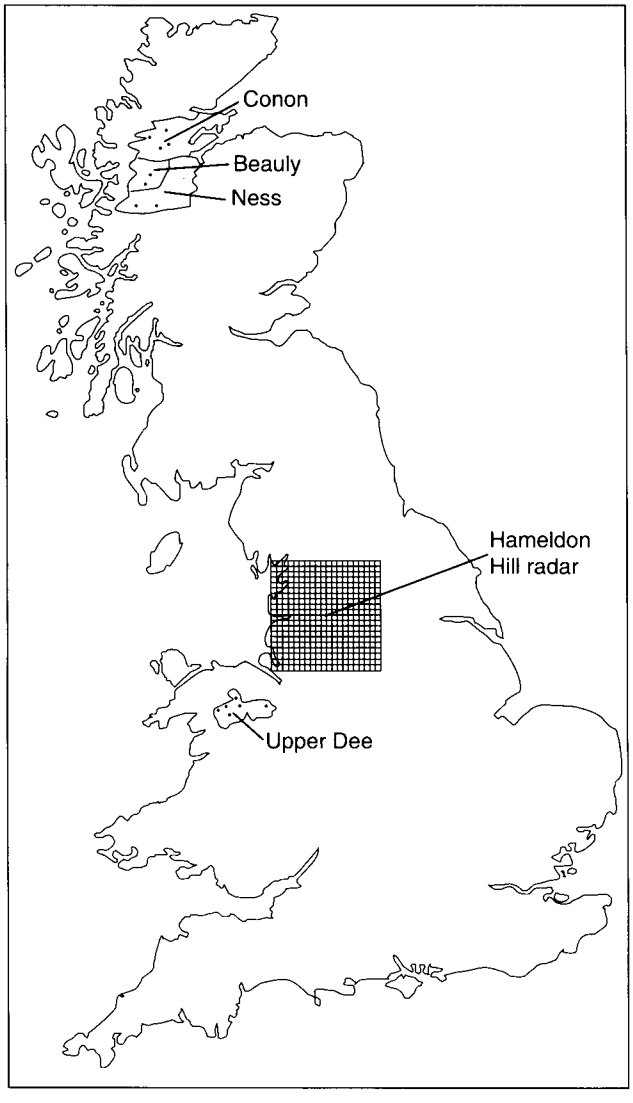

Figure 1. Upland regions for which data were available to the study.

2. Location of study areas and data available

Three predominantly upland areas (Fig. 1) were chosen to provide a cross-section of data types and durations.

In the Upper Dee catchment of north Wales, where average annual rainfall ranges from 900 to 2000 mm, data were selected for ten gauges from the dense network of 15-minute recording rain-gauges. The network was installed in the early 1970s as part of the Dee Weather Radar Project and 15-minute data are available for the period from September 1971 to March 1975 (Central Water Planning Unit 1977).

In north-west England hourly peaks-over-threshold (POT) data from the Hameldon Hill radar were used, which represent the areally averaged data used in the analysis. The radar field consisted of 400 five-kilometre grid squares, with hourly data available for 183 non-continuous rainfall episodes between 1981 and 1987. The average annual rainfalls in this area range from 750 mm to over 1500 mm.

In north-west Scotland the series of daily annual maxima were abstracted for 12 rain-gauges in the Conon, Beauly and Ness catchments. From all 12 gauges annual maxima data were derived for a range of durations for the 27-year period between 1961 and 1987. All three are complex, multi-reservoired systems and, as such, critical design storm durations are in excess of those for which the FSR technique is recommended (FSR II.6). Average annual rainfalls for the selected gauges in this region range from 1100 mm to over 2200 mm.

Tables I to III list the number of profiles extracted both annually and seasonally for north-west Scotland, north-west England (Hameldon Hill radar data) and the Dee data, respectively. Data in Tables I and III are annual and seasonal maxima; the Hameldon Hill radar data (Table II) were extracted using a POT criterion.

The distribution of extreme events through the year (in terms of the proportion of events in each season) is the same for all the data types, but changes with duration. As the duration increases the proportion of those events occurring in winter also increases, while the proportion in summer decreases. This is particularly true with the daily data interval, when the summer convective storm (typically producing only one or two days with an extreme rainfall depth) accounts for a higher percentage of the annual maximum events. These summer convective storms also produce some of the greatest intensities of rainfall over very short periods, which means they also tend feature in the much shorter duration summer maximum events.

Table I. Number of annual and seaonal profiles: daily rain-gauges in north-west England.

Duration	Total	Winter (DJF)	Spring (MAM)	Summer (JJA)	Autumn (SON)
3-day	523	146	71	123	183
5-day	523	149	58	136	180
7-day	523	172	61	113	177

Table II. Number of annual and seaonal profiles: hourly Hameldon Hill radar data.

Duration	Annual	Winter (DJF)	Spring (MAM)	Summer (JJA)	Autumn (SON)
4-day	1364	440	318	227	379
6-day	1180	379	277	191	333
12-day	865	280	215	125	245

Table III. Number of annual and seaonal profiles: 15-minute rain-gauge data from north Wales.

Duration	Annual	Winter (DJF)	Spring (MAM)	Summer (JJA)	Autumn (SON)
1-hour	512	110	34	175	193
2-hour	533	140	40	145	208
4-hour	524	154	43	122	205
6-hour	474	149	35	110	180
12-hour	354	124	27	65	138

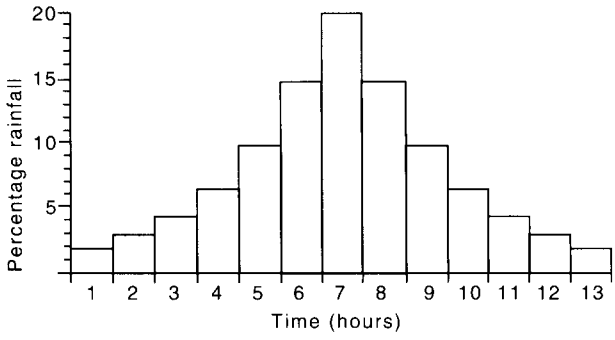

Figure 2. The winter 75% percentile profile using the FSR technique.

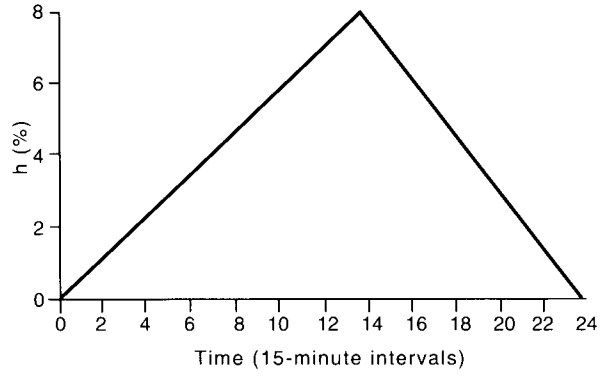

Figure 3. The winter 6-hour design profile for the Upper Dee data using the triangular moments method.

3. Methods of design profile derivation

Most current methods used to distribute design rainfall depths through time are objective techniques based on observed patterns of rainfall intensities. It is possible to distinguish three types of method currently in use around the world: those derived from averages of observed profiles, those involving the fitting of models to observed hyetographs, and more flexible empirical methods.

3.1 Averaging methods

Included in this category is the approach based on mass curves (for example, Huff (1967)), which produces dimensionless, cumulative plots of rainfall depth against time. Huff's method segregates storms according to the quartile in which the heaviest rainfall was recorded. Additionally in this category is the FSR technique which uses 24-hour storms, centred on the period of most intense rainfall. This produces unimodal and symmetrical profiles as illustrated in Fig. 2. The frequency of occurrence of profiles of varying sharpness is expressed through the use of percentiles. The winter, 75-percentile profile is generally recommended for flood design in predominantly rural catchments in the United Kingdom (FSR II.6).

These averaging techniques have the advantage of being relatively simple to implement and relate reasonably directly to observed rainfall events. The methods tend to produce design profiles that are so smooth and symmetrical, however, as to be unlike any of the input storm events, and their use becomes less realistic as the design duration increases.

3.2 Model-based methods

This group of methods uses a particular model to approximate the form of the observed profiles (for example, Keifer and Chu (1957), Yen and Chow (1980), Sutherland (1983)). The triangular model proposed by Yen and Chow uses a triangle to represent periods of non-zero rainfall and is fitted using a method of moments. The triangular hyetograph is defined by three parameters: the time to peak (a), the proportion of the duration occurring after the peak (b), and the peak magnitude (h). An example is shown in Fig. 3.

Although these techniques have been found to produce good results, the parameters vary with location and duration and prove difficult to generalize. In particular these methods do not take account of the variability in the observed storm events. The triangular-moment method (Sutherland 1983) was designed to be applied to real storms and not fixed duration events, so it is unclear how it may be used in design applications.

3.3 Empirical methods

The third group of methods includes the so-called average variability method, developed in Australia by Pilgrim *et al.* (1969). The method was developed to produce design profiles for durations of between 10 minutes and 72 hours and seeks to characterize the mean variability of rainfall intensity during observed periods of heavy rain. The main advantage of the average variability method is that the mean position of the observed peaks is conserved. This allows the design profiles to be asymmetrical and multipeaked, a feature evident in observed profiles due to the inherent variability of the rainfall process itself, when observed at a stationary point. A 6-hour profile produced by the average variability technique is shown in Fig. 4. The average variability method can be seen to provide more detail than the other methods (Figs 2 and 3). A negative skew is apparent in both Figs 3 and 4, although this is less obvious in the triangular profile. Because the average variability method provides a rainfall depth for each 15-minute interval, a more detailed profile is produced.

A somewhat similar approach was developed by the SOGREAH group in France. The method produces a median pattern centred on the period of most intense rainfall (Hall and Kneen 1973). More recently, Srikanthan and McMahon (1985) have developed a technique to take account of the persistence from one sub-duration to the next, especially for durations of less than one day. As all observed profiles are centred on the period of heaviest rainfall, some data from the more unusual events are discarded when using this technique.

4. Results and discussion

The results presented in this paper concentrate primarily on the average variability method and compare the effects of data type, data interval, season, duration and areal averaging. The discussion section is divided into two parts: the first dealing with the short-duration profiles (up to 12 hours), the second looking at the much longer design profiles (up to 11 days)

4.1 Short-duration design profiles

Figs 5 and 6 illustrate the design profiles produced using the average variability technique for the 4-hour

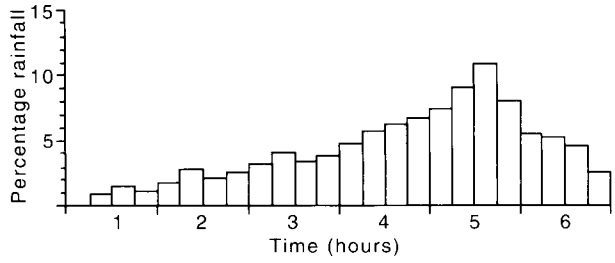

Figure 4. The winter 6-hour design profile for the Upper Dee data produced using the average variability method.

duration. The profiles were split according to season with winter comprising December, January and February, and summer defined as June, July and August. Figs 5(a) and 5(b) compare the summer and winter results from the 15-minute Dee data. Close inspection reveals that, not only is the variability between each sub-duration greater in the summer than in the winter, but there is also greater variability within each sub-duration; the latter is represented by the error bars which corresponds to the inter-quartile range. This range has been used rather than the standard deviation as the distribution of depths within the very low sections of the profile is far from normal. However, the factorial standard error cannot be used as the depths within the peaks of the profile approximate a normal distribution, hence the inter-quartile range has been shown.

A statistical analysis of the input profiles showed that those from the Upper Dee were not significantly different from those derived from the radar data at the same durations. This made it possible to compare the point data from the Dee catchment with the areally averaged Hameldon Hill radar data. Fig. 6 shows the summer and winter average variability design profiles produced using the hourly radar data for the 4-hour duration. The most notable feature of Figs 5 and 6 as a group is the extent to which the Dee point data are in agreement with the radar data. Table IV compares hourly depths for the Dee data (obtained by summing the four 15-minute intervals within each hour) with those for the radar data. While the actual percentages are not the same, the broad patterns are very similar, with the more peaky nature of the summer profiles and the negative skewness being reproduced in both data types.

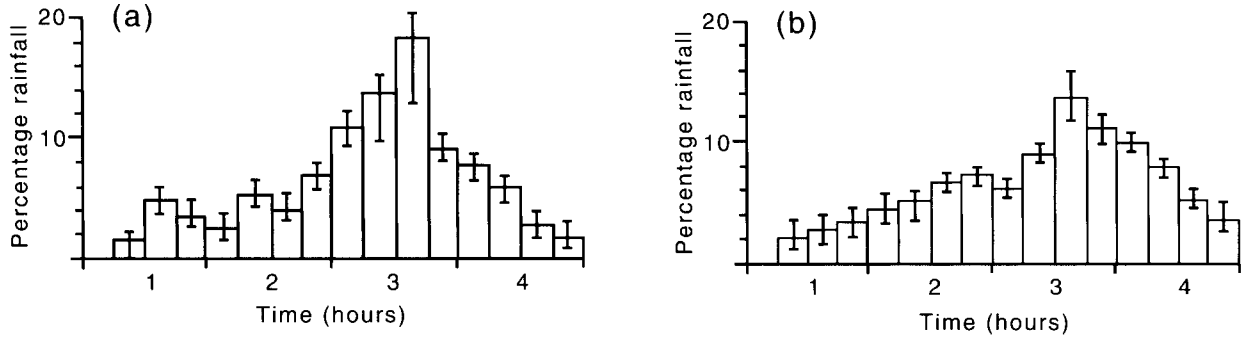

Figure 5. The 4-hour average variability design profile using Upper Dee data, (a) summer, and (b) winter.

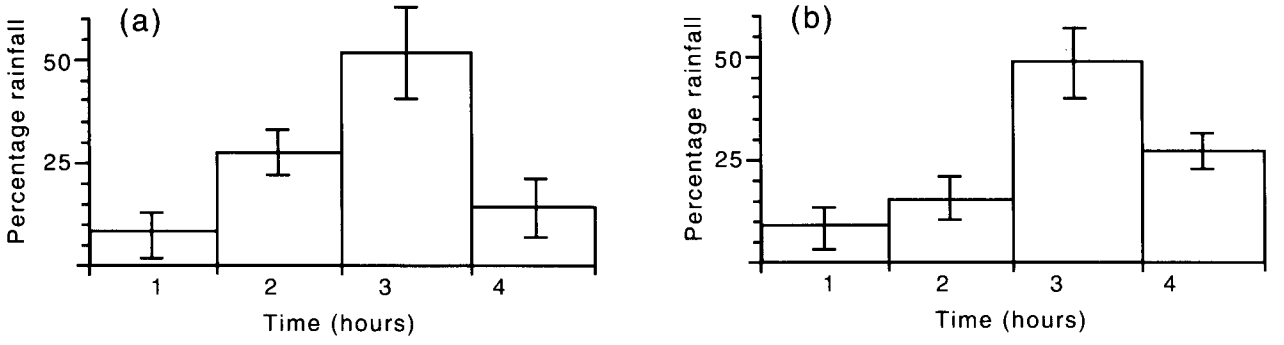

Figure 6. The 4-hour average variability design profile using Hameldon Hill radar data, (a) summer, and (b) winter.

Table IV. Comparison of hourly totals, in percentages, for point (Dee) and areal (Hameldon Hill radar) data for the 4-hour duration.

Time interval	Winter (DJF)		Summer (JJA)	
	Radar data	Dee data	Radar data	Dee data
1	9	8	8	9
2	16	24	27	19
3	48	40	51	53
4	27	28	28	19

Table V. Comparison of hourly totals, in percentages, for point (Dee) and areal (Hameldon Hill radar) data for the 12-hour duration.

Time interval	Winter (DJF)		Summer (JJA)	
	Radar data	Dee data	Radar data	Dee data
1	0.4	0.3	0.5	3.9
2	1.5	2.8	5.0	11.6
3	3.1	7.3	33.9	9.7
4	13.5	15.6	20.1	7.3
5	10.2	11.6	9.4	3.0
6	31.3	22.2	12.9	1.7
7	19.3	9.1	2.9	0.4
8	5.7	13.6	1.5	1.2
9	7.7	9.5	2.1	6.7
10	4.1	4.8	3.8	29.2
11	2.3	1.3	7.0	16.6
12	0.8	1.9	0.9	8.9

Table V and Figs 7 and 8 show the corresponding results for the 12-hour duration and show many of the features of the 4-hour profiles. The summer profiles are again more variable from interval to interval and within intervals. The shape of the design profiles at this 12-hour duration are different, however. The summer radar data produce an early peak, while a late peak is evident in the summer Dee data, although both profiles display double bursts. This difference in the shape of the two profiles may arise because of the difference between the areally averaged radar data and the point Dee data, although this is not apparent in other seasons or at other durations. Given the similarity between the 4-hour profiles (for both seasons) and the 12-hour winter profiles, the difference probably occurs because of the nature of the available radar data. Although hourly radar data are held between 1981 and 1987, the record is far from complete. Very often the full 12 hours either side of a selected 12-hour event were not available, so it is unknown whether or not the event was centred correctly, or indeed whether the event was the most extreme.

The important feature to note from Figs 7 and 8 is the multipeaked nature of the design profiles. The average variability method generally produces multiple peaks once the number of data intervals exceeds about four. This may be at durations of greater than four days with daily data, or even at the 2-hour duration with 15-minute data. This flexibility is not found with any of the other methods and reflects the variability of the rainfall process.

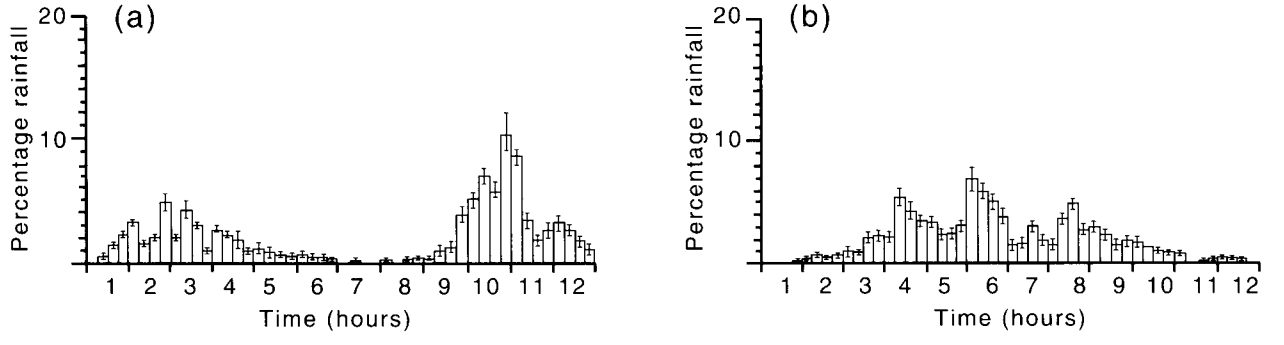

Figure 7. The 12-hour average variability design profile using Upper Dee data, (a) summer, and (b) winter.

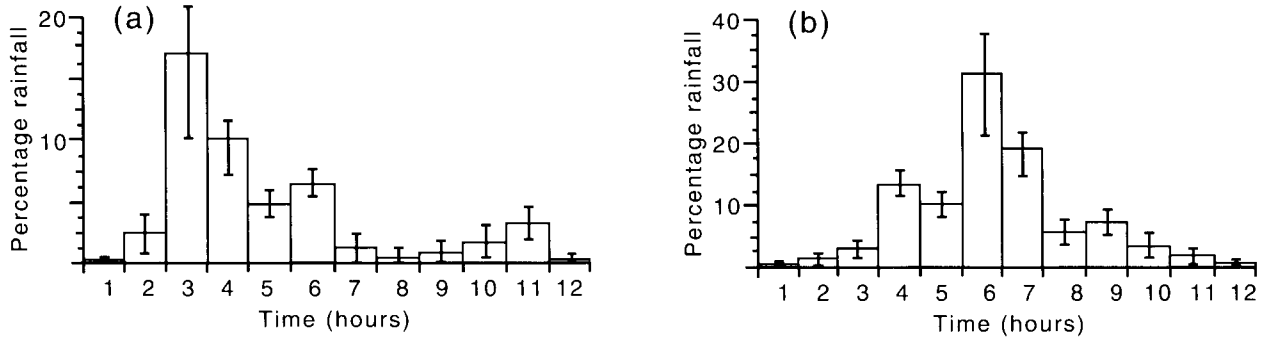

Figure 8. The 12-hour average variability design profile using Hameldon Hill radar data, (a) summer, and (b) winter.

4.2 Long-duration design profiles

Fig. 9 illustrates the results from applying the average variability method at the 3-, 7- and 11-day durations using annual data (all the annual maxima events were included) from north-west Scotland. For comparison, the results of the alternative method (Srikanthan and McMahon 1985) for the same durations are also shown. The 3-day profiles of the two methods are very similar, as indeed they are for the SOGREAH, FSR and modelling methods, being broadly triangular. Thereafter the similarity between methods ends. The average variability method produces a design profile at the 7-day duration

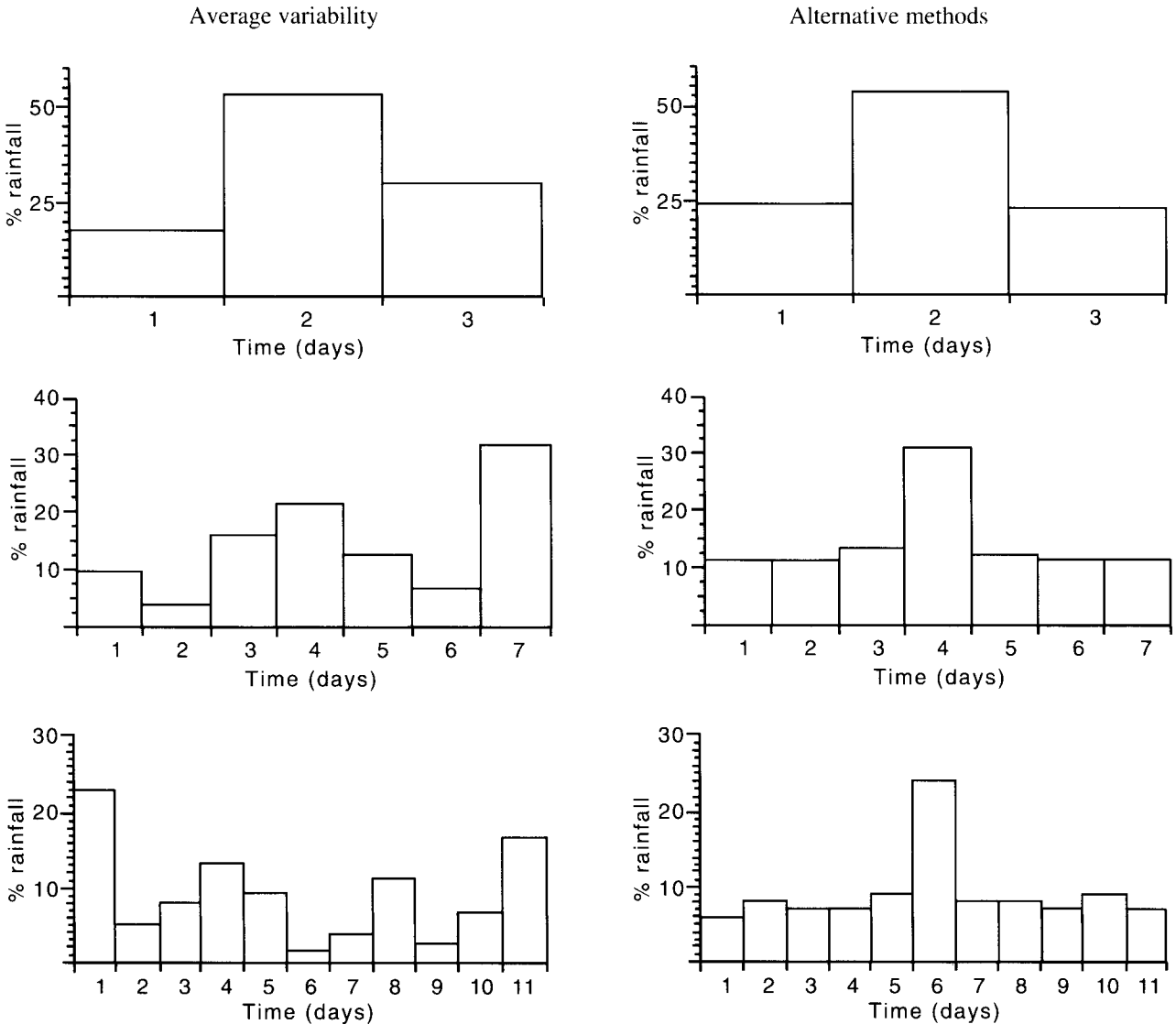

Figure 9. Design profiles for the 3-day (top), 7-day (centre) and 11-day (bottom) durations for north-west Scotland produced using the average variability and 'alternative' methods.

with three distinct peaks (in fact multiple peaks first appear at 4 days). At 11 days there are four obvious peaks. In contrast, the shape of the profiles produced by the alternative method remain the same throughout, being unimodal and symmetrical.

It is the apparent physical realism of the average variability design profiles that is so important as the durations move beyond a few days. Section 4.3 describes a typical annual maximum event from one of the Scottish rain-gauges and so highlights the intensely variable nature of daily rainfall. The event chosen is centred on 16 December 1966 when the daily rainfall total was well over 100 mm at the chosen gauge. Fig. 10 illustrates the 15-day profile centred on the 16th.

4.3 An example

The initial, fairly small peak on days 1 and 2 of the profile (corresponding to 9 and 10 December) represents the cold front of a relatively weak depression that had cleared Scotland by the 11th. Within four days a second, much deeper system passed over northern Scotland. This system was occluding as it crossed and deposited copious amounts of rain during the 16th and 17th producing the dominant 2-day peak in the profile (this 2-day rainfall was so extreme that the same two days appear in the annual maximum profiles for all durations from two to 12 days at this rain-gauge). The cold front associated with this depression was left trailing over the United Kingdom in a strong westerly flow. This led to the development of a wave depression that crossed Scotland on 21 and 22 December and accounted for the third peak in the profile (Fig. 10).

The above description is for only one annual maximum event, but at all durations greater than a few days a similar multiple peaked shape is evident. Given the inappropriate nature of the recommended FSR design profiles for these very long durations and the importance of these events in some slowly responding, multi-reservoired catchments, engineers in Scotland have developed their own local method of deriving rainfall profiles for design applications (Jarvis, personal communication).

The nature of the average variability method means that, from any number of extreme rainfall events, it can objectively produce a long-duration design rainfall profile of a 'realistic' form, rather than relying on just a few selected extreme events, as does the rather subjective method currently used for longer durations in Scotland. It is the flexibility and physical realism of the average variability profiles that suggests this is a more appropriate method for deriving design rainfall profiles, especially at the longer durations, although its performance within the overall design context is yet to be compared with the other methods.

5. Conclusions

Design rainfall profiles have been derived using a number of data sets from the upland areas of the United Kingdom. Several methods were used in order to reassess the applicability of the FSR method, especially at longer durations.

The observed profiles are generally multipeaked for durations longer than four times the data interval, as might be expected under a simple scaling assumption (Dwyer and Reed 1993). For instance, the daily profiles have more than one peak at durations greater than four days, while the 15-minute profiles exhibit multiple peaks at durations greater than one hour. It seems appropriate that any design profile should bear some resemblance to the profiles used in its derivation and only the average variability method is flexible enough to allow multiple peaks in the design profiles.

The comparison of the seasonal design profiles produced using the average variability method suggests that there is greater variability in the summer. This is evident across all data types and all durations, although it is less obvious in the Scottish annual maximum data. This pattern is also to be found in the observed profiles. The reason for this seasonal difference is due to the rainfall process itself with the (more temporally variable) convective rainfall responsible for a significant number of the summer extreme events and the (more temporally persistent) frontal rainfall being totally dominant during the winter.

Specific recommendations for the use of design rainfall profiles within a rainfall run-off method of flood estimation fall beyond the scope of this paper. It has been

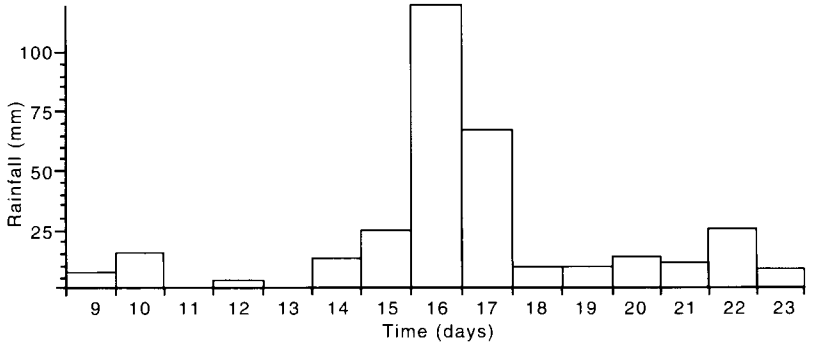

Figure 10. The 15-day profile for gauge 713571 in north-west Scotland, centred on 16 December, 1966.

shown that the application of the average variability design profiles, as opposed to the traditional bell-shaped profiles, produce lower peaks in the design hydrographs (because of the greater distribution of the rainfall) and hence the use of the unimodal profiles tends to produce a somewhat conservative design estimate (Aron and Adl 1992). It is the view of the authors that the average variability method (Pilgrim *et al.* 1969) offers a simple and flexible method of design profile derivation that appears to cope well with the great natural variability of the rainfall process.

Acknowledgements

The analysis presented in this paper forms part of a wider study of the spatial and temporal variability of extreme rainfall events in upland areas of the United Kingdom, commissioned by the UK Department of the Environment (contract no. PECD7/7/190). Strategic research on flood and rainfall estimation is funded by the Ministry of Agriculture, Fisheries and Food. The assistance of Mr R.M. Jarvis of Scottish Hydro-electric plc in providing details of current design practice is gratefully acknowledged.

References

Aron, G. and Adl, I., 1992: Effects of storm patterns on runoff hydrographs. *Water Resour Bull*, **28**, 569–575.

Central Water Planning Unit. 1977: Dee weather and real time hydrological forecasting project. Reading, Central Water Planning Unit.

Dwyer, I.J. and Reed, D.W. (1993): Using effective fractal dimension to correct the mean of annual maxima. Submitted to *J Hydrol.*

Hall, A.G. and Kneen, T.H., 1973: Design temporal patterns of storm rainfall in Australia. *In* Proceedings of Hydrology Symposium, I.E. Aust., Perth 1973.

Huff, F.A., 1967: Time distribution of rainfall in heavy storms. *Water Resour Res*, **3**, 1007–1019.

Keifer, C.J. and Chu, H.H., 1957: Synthetic storm pattern for drainage design. *J Hydraul Div ASCE*, **83**, 1332-1 – 1332-25.

Natural Environment Research Council, 1975: Flood Studies Report (five volumes). London, NERC.

Pilgrim, D.H., Cordery, I. and French, R., 1969: Temporal patterns of design rainfall for Sydney. *Civ Eng Trans I.E. Aust*, **CE11**, 9–14.

Srikanthan, R. and McMahon, T.A., 1985: Temporal storm patterns re-examined. *Civ Eng Trans I.E. Aust*, **CE27**, 230–237.

Stewart, E.J. and Reynard, N.S., 1991: Rainfall profiles for events of long duration. *In* Proceedings of the third National Hydrology Symposium, University of Southampton.

Sutherland, F.R., 1983: An improved rainfall intensity distribution for hydrograph synthesis. University of the Witwatersrand, Water Systems Research Programme, Report No. 1/1983.

Yen, B.C. and Chow, V.T., 1980: Design hyetographs for small drainage structures. *J Hydraul Div ASCE*, **106**, 1055-1076.

World weather news — February 1993

This is a monthly round-up of some of the more outstanding weather events the month, three preceding the cover month. If any of you, our readers, has first hand experience of any of the events mentioned below or its like (and survived!), I am sure all the other readers would be interested in the background to the event, how it was forecast and the local population warned.

These notes are based on information provided by the International Forecast Unit in the Central Forecasting Office of the Meteorological Office, Bracknell and press reports. Naturally they are heavily biased towards areas with a good cover of reliable surface observations. Places followed by bracketed numbers, or areas followed by letters, in the text are identified on the accompanying map. Spellings are those used in The Times Atlas.

South America

Over the 7th a vigorous depression brought unseasonal cold, heavy rain and winds gusting to 50 kn to Uruguay (U) and Argentina (A): at least 15 are believed to have been killed. There was severe flooding around Buenos Aires as both the Rivers Parana and Plate burst their banks (the latter was at its third highest mark this century). The winds raised big seas and a storm surge caused a lot of coastal flooding and about $50m damage; the port of Mar del Plata was closed until the 10th.

On the 11th, heavy thunderstorms occurred SW of Sao Paolo (1), Brazil, where the town of Parangua had 209 mm in only six hours. Further north in the Colombian capital, Bogota, after a spell of average weather, the night minimum temperature fell to +1 °C; this is 4 °C lower than the previous record.

North America

New York (3) started the month with the passage of a cold front that knocked temperatures down to −13 °C with a near-gale from the north. All things are relative — on the 3rd there were reports that in Fairbanks (4), Alaska, where the AVERAGE for February is −13 °C, the temperature got down to the record low for the month of −50 °C: meanwhile winds of nearly 100 kn had closed the port of Valdez. It must have been cold over Canada as well, because the port of Montreal was badly affected by dangerous ice-jams on the St Lawrence Seaway for the first three weeks of the month.

Los Angeles (5) average rainfall is 66 mm this month; 86 mm fell during the 7th and 8th. However I saw no reports of flooding in California until the 18th. Then a storm deposited around 75 mm on the saturated ground.

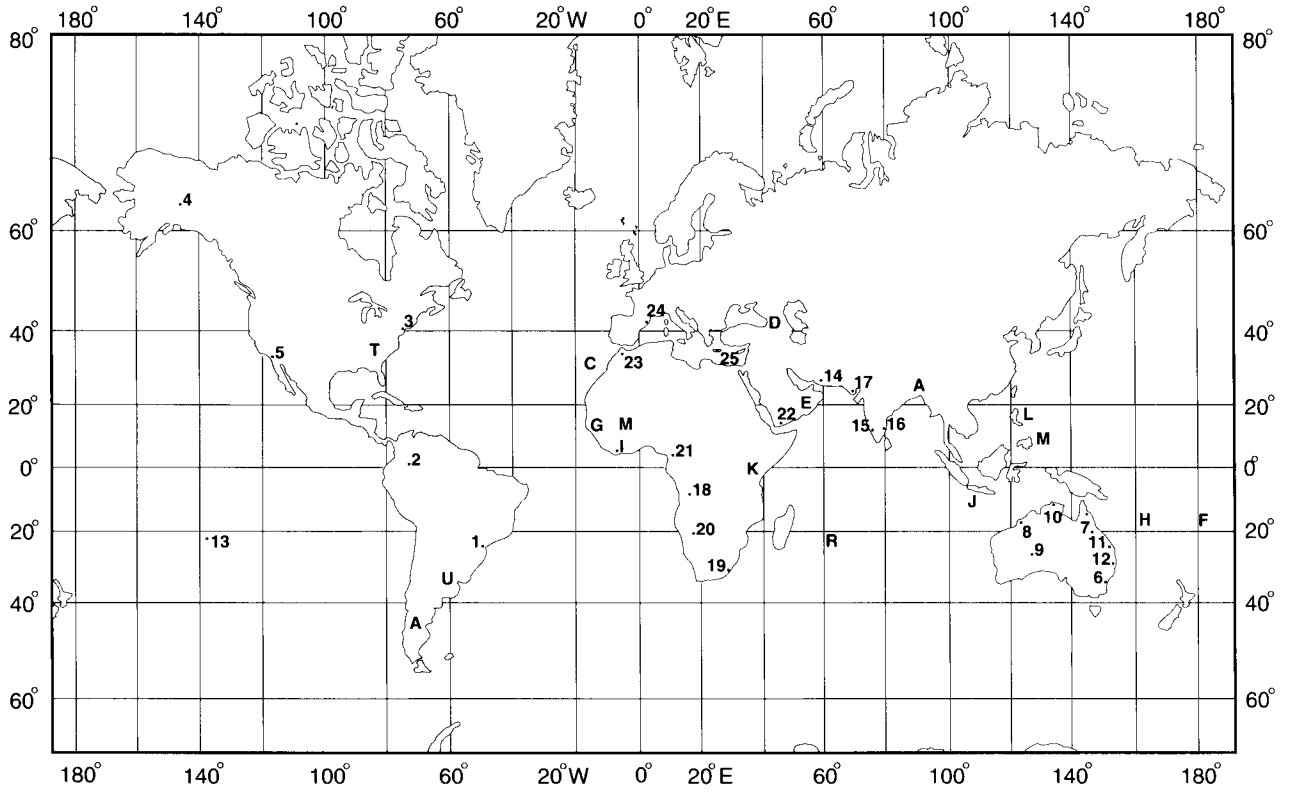

Location of places mentioned in text

Some 100 hillside homes had to be abandoned as the ground started to slip, and floodgates were opened at 13 dams which were in danger of being overtopped. It seems that there has been nearly 600 mm of rain in Los Angeles since the storms started in December (the long-term average would be 250 mm but for the last six years it has been 150 mm), their drought is now officially over!

It was much the same story on the 24th when more heavy rain (and 20 cm of snow in the hills) caused two lanes of Interstate Highway 5 to buckle in Los Angeles County; they were to remain closed for the rest of the month. The railway line from L.A. to San Diego was closed as well (until 9th March) by a landslide which included parts of four houses. Meantime over in Arizona the Gila River, almost dry not long ago, had become a raging torrent, spilling over nine dams and threatening to rise higher as mountain snow started to melt. Many bridges over the river were unusable because of the water level. Shallow lakes in the area were rapidly filling and threatening shoreline developments. In all damage reached about $200 m.

Between these last events, on the 21st, there were severe thunderstorms over the eastern State of Tennessee (T) where there were several tornadoes and baseball-size hail.

Australasia

A large tropical depression over Western Australia has provided some newsworthy weather for the start of the month; the south has had blistering heat and the west remarkable rainstorms. The heatwave brought temperatures of up to 42 °C in Sydney (6) on the 4th (this is can be compared with the February average maximum of 26 °C: twelve deaths have been attributed to the heat. On the 5th things were back to normal with a maximum of 26 °C. The lack of reports of drowning elsewhere is surprising. Among the reports received in the first few days of the month were Cooktown (7), north Queensland, 157 mm in 6 hours, part of 255 mm in 48 hours; Lagrange (8), Western Australia, 139 mm in 24 hours; Carnegie (9), central W. Australia, 290 mm in 24 hours; Milingimbi (10), in the north of Northern Territory, capped them all with 304 mm in 24 hours to 0100 on the 5th.

Cyclone 'Oliver' temporarily closed the Port of Hay Point, Mackay (11), Queensland, on the 8th as it passed nearby. Reports of heavy rain kept coming in during the month, one station near Brisbane (12) had 190 mm in 24 hours on 2nd.

Heavy rain does not require a continental land mass to trigger it. The island of Mururoa (13) in the far east of Polynesia, had 412 mm in the four days to the 8th (the monthly average is 130 mm). At times the wind approached 30 kn and visibility reduced to fog limits. This could have been due to the early stages of T/S 'Mick'. Later in the month T/S 'Polly' developed in the New Hebrides (H) and the island of Taro in the neighbouring Solomons got 103 mm on the 24th. A few days

later on the 27th, and about 1000 miles east of 'Polly', there were amazing downpours in the Fijian (F) archipelago. Nandi Airport recorded consecutive 6-hourly totals of 22, 93, 90 and 77 mm; the total of 284 mm is practically the average February total.

Asia

Heavy rain at the end of January and the beginning of this month caused much misery in the south-east. Mindanao (M) declared a state of calamity because of the severe flooding in the north of the island after two weeks of heavy rain; about 23 are reported drowned. Jawa (J) has featured much in these notes since they began: again flash flooding and landslides claimed at least 80 lives in the first few days after 'heavy' rain in central and eastern parts of the island. Jakarta collected 250 mm between the 4th and 8th; further east, Tegal on the north coast had 130 mm in 24 hours on the 7th. Parts of Semarang were under 4 ft of water and the airport was closed. Road and rail traffic was severely disrupted and as many as 0.5 million were evacuated to higher ground. In Jakarta traffic was almost at a standstill, and in Kudus and Demak provinces about 5000 had to live on their roofs for three days! Damage runs to at least $23m. At sea 10 were drowned but 79 saved when a vessel foundered in heavy seas.

Further east the island of Timor managed 223 mm in 12 hours to the 14th. On the 2nd there was a sinister development in the south-east of Luzon (L) when the volcano Mount Mayon threatened a major eruption. Initially there were a dozen deaths from falls of red-hot rocks, but then heavy rain mixed with fresh ash to cause 'lahars' killing another 50 or so. A considerable area around was then evacuated and there were eruptions on and off for the rest of the month. The biggest explosion was on the 12th which sent ash 6 km upwards.

Heavy rain at the start of the month brought flooding to much of western Iran by the 8th, with some 150 000 homes damaged or destroyed: 15 000 km of roads were reported washed away along with 1000 bridges and 250 000 head of livestock. The human toll is believed to be about 500 killed, at least 225 of these in Bandar Abbas (14) which was particularly badly hit. Floodwater and avalanches were still causing disruption on the 25th.

Indian subcontinent

High temperatures in the south were the early focus of attention; Colombo, Sri Lanka, started the ball rolling with a new February record of 36.2 °C on the 4th: this was repeated a few days later, and on the 15th 36.6 °C was a new record on the mainland at Coimbatore (15), Kerala. The 16th brought near-record 36s in Gujarat, and 38.8 °C to Nellore on the east coast just north of Madras (16) on the 18th: then the emphasis switched to rain.

In Assam (A) and north-east Bangladesh there was a 'freak' storm on the 19th which produced flash flooding that killed eight and injured 500, destroyed 15 000 homes and made 70 000 homeless. The floods destroyed the main railway bridge link in the area. Storms of this type are more usual in April rather than so early.

Heavy rain fell in south Pakistan on the 24th/25th leading to four deaths around Karachi (17) which was virtually paralysed. The cold front triggering the storm brought maximum temperatures of only 10 °C in its wake. Despite the chaos, the local meteorological service is quoted as describing the 12 mm of rain 'as normal for February' (*I think 'as the normal for the whole of February' was meant*). Bhuj-Ruramata by the Gulf of Kutch had 22 mm in 3 hours (this month's average is 4 mm and a properly wet February day is expected once in 120 YEARS).

Africa

Man's arbitrary division of the year into months is sometimes inconvenient when the weather forgets to recognize them. In Kenya, the weather of January had effects which spilled over into February, as reported by the World Climate Programme of WMO, quoted below.

'The perception among Kenyans that January is a dry month is unfounded. Six months of the year are wetter but, on average, there are five drier months. In the past 48 years there has been zero rainfall at Nairobi on only five occasions. Most of January's rainfall occurs during a couple of wet spells, often thundery, which add up to 50 mm on average at Nairobi. The mountain areas of Kenya are much wetter, for example, Kimakia Forest Station on the Aberdare Mountain Range averages twice the rainfall of Nairobi. Yet Nairobi recorded 237.2 mm in 1993. It rained on 21 days with a maximum of 39.4 mm falling on the 16th. Rain was widespread. Amboseli National Park, a prominent tourist attraction boasting all-weather roads, was closed at the end of the month because of flooding.

'Nothing remotely like this had hit Kenya before except in 1957 when 235.2 mm was recorded, mostly from violent storms during the last ten days of the month.

'A new meteorological record is always of interest and the situation could be described as a 1-in-25-year event. Records are insufficiently long to confirm anecdotal estimations that the event of 1957 was, until this year, unique in the century and about double the next highest January rainfall recorded or remembered.'

Amboseli was still closed during the first week of February.

Heavy rains were still around in this month. notable falls were 100 mm in about 6 hours in Kinshasa (18), Zaire, and Newcastle (19), South Africa, on the 8th. Rundu (20) in north-east Namibia (February average 133 mm) managed 183 mm in the week to the 18th including 77 mm in 3 hours. In the Cameroon, Douala's (21) 99 mm on the 18th easily beat the previous 24-hour record for this month. Two days later just round the Gulf in Ivory Coast, 82 mm in a day was twice the monthly average. Similar wetness affected Zimbabwe on the 21st when thunderstorms dropped about 100 mm on several places in the course of the day.

Temperatures were extraordinary in quite a few places, noteworthy reports include 41.6 °C at Banjul, The Gambia (G), on the 10th, when a light south-easterly helped break the annual extreme record of 40 °C. On the 22nd Tombouctou, Mali (M), had a maximum of 37 °C; then a cold front passed south and next day it only reached 28.5 °C while, 200 miles to the east Gao, got 99 mm of rain in the middle of its dry season. N'Guimi at the north-west end of Lake Chad reached 41.7 °C on the 27th, 1.7 °C above the previous record for this month. South Africa has also had a heatwave, temperatures exceeding 40 °C in several places in the middle of the month.

The Canary islands (C) had a force 7 northerly on the 27th, during which the 1000-tonne *Isla de la Gomera* sank off the Moroccan coast while on passage from Cadiz to Las Palmas: most of the crew of 15 were rescued. On the other side of the continent in St Denis, Réunion island (R), there was some of the type of weather not mentioned in the holiday brochures: 353 mm of rain over the last two days of the month and 606 mm over the last eight days. This was no fluke! Earlier in the month there had been 331 mm in the five days to the 17th (including 173 mm on the 16th): my old reference book gives the February average rainfall as 1400 mm for a gauge nearby.

Europe and Arabia

Severe storms over the Kola Peninsula (K) on the 2nd brought down powerlines near a nuclear power station leading to its temporary shutdown. Large areas of Murmansk were without electricity; trains stopped running and some factories had to close. The same storm raised waves of more than 7 m in the northern North sea, temporarily closing down the oilfields there and driving the mv *Rhino* aground south of Bodø where she stayed fast for several weeks; her crew of eight were rescued by helicopter.

This is the prime month for cold fronts to work their way right down the Arabian Peninsula; the effects can be spectacular round the Gulf, but are usually very short-lived. This year it seems to have been different. On the 1st, Dharan (February average 15 mm) kicked-off with 40 mm in 6 hours. Similarly Bahrain had 24 mm in 12 hours on the 4th, Doha had 18 mm and Khaber, north Saudi Arabia capped them all with 96 mm. Then it was the turn of Emirates (E). Here there had been sandstorms with temperatures up to 30 °C on the 4th, then came the rain with totals of around 75 mm in 36 hours in many places (top of the table was Ras al Khaimah with 129 mm) with temperatures down to about 23 °C: on the 6th, under overcast skies, they were barely reaching 16 °C. Over the period 6th to 9th there were sketchy reports of serious flooding in South Yemen which killed at least ten. In Aden (22), serious damage to homes and 50 cars wrecked was noted. (I spent two years in Aden and have seen the effect of 20 mm of rain in a morning: it would not require much more to have this effect.)

Staying on the boundary of the region, in mid-month a story emerged from Dagestan (D) in the Caucasus (see November weather notes). It seems that winter snowfalls have been of unprecedented length making farming almost impossible, and supplies to populated areas are becoming critical.

At the other extreme of this region, by the Strait of Gibraltar, a levanter was diverted south-westwards by a small low over the Atlas and the forced uplift gave Tetuan (23) 168 mm of rain in four days to the 8th (monthly average is 107 mm); the neighbouring towns of Cueta and Melilla had just over 40 mm each in the same period.

High winds in the North Sea were back in the news on the 21st when winds of near hurricane force, accompanied by heavy snow showers, forced the operators to part an accommodation platform (with nearly 500 aboard) from its oil rig about 10 miles south-east of Aberdeen — the waves threatened to batter the two together. Potentially fatally confusing were problems experienced by the *Nordqueen* and *Norqueen*. The former, a 500-tonne grain carrier suffered engine failure and capsized after its crew of nine had been rescued by helicopter: the latter was in collision with a trawler in a mere force 7. Ill-timed engine failure also caught the 2300-tonne *Linda Buck* off a lee shore and she was driven aground near Terschelling. It was not much safer on land: more than 600 people were evacuated as a precaution as a storm tide, described as of a 'once in decade' height, caused some East Anglian sea defences to collapse. The sea was only one metre below the level of the 1953 catastrophe; in Lowestoft the water reached 2.2 m above the astronomical prediction and jammed the bridge to the inner harbour. In Ostend a 45 metre-high crane was blown down damaging cars and buildings in the vicinity, and dropping a 3-tonne weight through a bedroom, just missing the occupant.

As the cold air swept south, a low formed south of the Alps winding up the mistral. It had been up to storm force on the 19th for a time before dropping away temporarily. Next day, the 21st, it was back full blast with Cap Béar (24, near Perpignan) clocking 68 kn at one stage before easing at midday down to 54 kn gusting 76 kn. Off Palermo the gale broke the moorings of the 2500-tonne *Gidara* and drove her onto the rocks. A few days later, on the 26th, an Aegean force 7 drove a ferry onto a sandbank off the Cycladean island of Sifnos (25).

About 20 cm of wet snow fell at Kargaburan in Turkey on the 25th: shortly afterwards the 620 ft LORAN transmitter tower there collapsed.

February tropical storms

This is a list of tropical storms, cyclones, typhoons and hurricanes active during February 1993. The dates are those of first detection and date of falling out of the category through dissipation or becoming extratropical. The last column gives the maximum sustained wind in the storm during this month. The maps show 0000 UTC positions: for these I must thank Julian Heming and Susan Coulter of the Data Monitoring group of the Central Forecasting Office.

No	Name	Basin	Start	End	Max. (kn)
1	14P	AUS	26Jan.	7Jan.	35
2	Lin	AUS	31Jan.	4 Feb.	65
3	Oliver	AUS	4 Feb.	12 Feb.	110
4	Mick	AUS	5 Feb.	9 Feb.	45
5	Nisha	AUS	12 Feb.	16 Feb.	60
6	Finella	SWI	13 Feb.	15 Feb.	75
7	Oli	AUS	15 Feb.	18 Feb.	50
8	Gracia	SWI	21 Feb.	23 Feb.	30
9	H1	SWI	24 Feb.	26 Feb.	40

Basin code: N — northern hemisphere; S — southern hemisphere; A — Atlantic; EP — east Pacific; WP — west Pacific: I — Indian Ocean; WI — west Indian Ocean; AUS — Australasia.

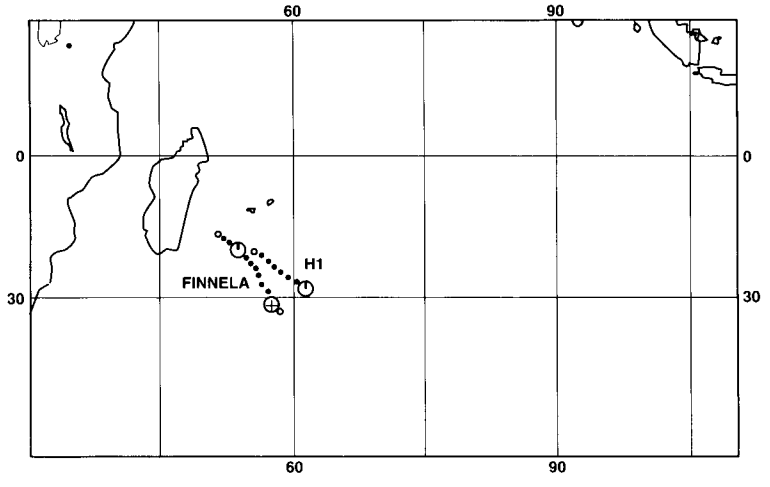

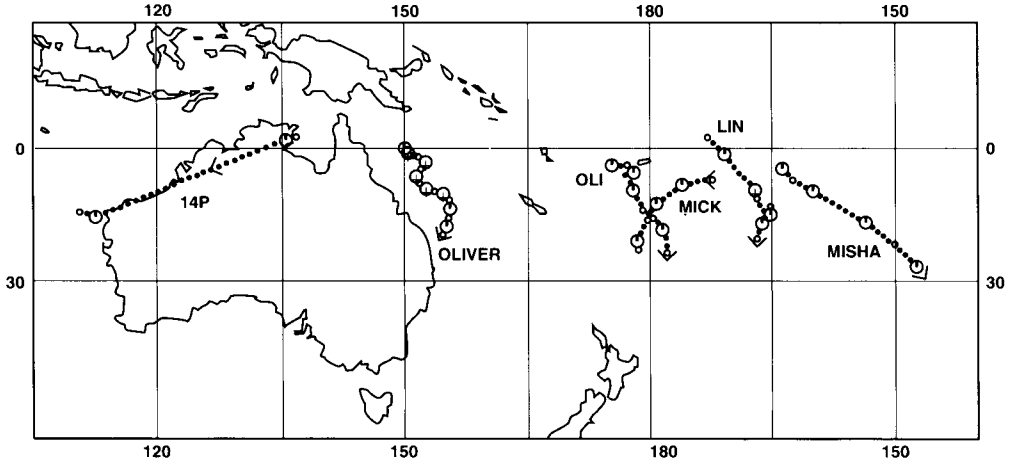

Obituary

Martin Morris

After a struggle with cancer Martin Morris passed away on Tuesday 5 January 1993 in Hammersmith Hospital. Since July 1992, Martin had been Head of the Central Forecasting Office (CFO), a newly created post in which he hoped bring his expertise and ideas in forecasting to fruition. Martin was no stranger to the Central Forecasting Office as he had been Assistant Director of Central Forecasting in the five years leading up to Agency — a period when techniques where changing to accommodate the more sophisticated modelling of the atmosphere. Martin developed ideas which assisted the forecasters in the CFO to extract from the model as much information as they could using model diagnostics. Martin felt that the whole of forecasting revolved around the omega equation and insisted that if only the forecasters could understand this they would have the key to success. With this in mind he strove to provide the forecasters with the derived fields of advection and ascent from the model and encouraged them to link these diagnostics with the real world as indicated by real data and especially satellite imagery.

Martin Morris was a forecaster at heart and an ardent ambassador for ensuring that our prestige was well known. When on the Senior Forecaster's roster in the early 1970s, the days of the 10-level model, he would tear the model to pieces when it came up with 'unmitigated rubbish from north to south and east to west'. But on a later posting as Head of the London Weather Centre he was quick to see the value of the numerical model to the rapidly expanding oil industry and he extolled the plus points of the model to those involved.

Born in the West Riding of Yorkshire in March 1937, Martin developed an early interest in Meteorology taking observations while at the Silcotes School near Wakefield. He entered the Meteorological Office in 1954 as an Assistant but while doing his National Service he realized that his ambition to forecast would not be possible unless he went for higher qualifications. With this in mind he obtained his degree in Applied Mathematics at the City University and so entered his scientific career in the Office. Soon after, he was posted to Cyprus and while there he had time to ponder the atmosphere and set about drafting chapters for a possible book. Although the text was never published it formed the vehicle for his thinking in the following years.

He was Assistant Director of Met O 7 (Public Services) for four years following his spell at London Weather Centre. In 1988 he returned to Central Forecasting as Assistant Director. One of his particular achievements during that period of four years was the work he did in making known the success of the Bracknell model in predicting tropical storms. As a direct result of his efforts routine messages are now sent to Guam, Beijing, Melbourne, Pretoria and Mauritius advising them of the model output relating to tropical cyclones in their areas of responsibility. Another achievement during that time was the setting up of a Specialist Group on Weather Forecasting within the Royal Meteorological Society. Martin also used every opportunity to promote the work of the Meteorological Office, giving up valuable time to give talks to groups ranging from after dinner speeches to the informal talk to a group in a local hall.

During his career Martin published several articles and was co-author of a book on climate. His interest in the North Sea oil industry while at London Weather Centre brought him into contact with the E & P Forum, an interest he maintained until his death. This interest in the oil industry resulted in an article in the *Meteorological Magazine* dealing with the accuracy of the wind and wave forecasts issued by London Weather Centre. The advection of warm air on the forward side of an upper trough to the west of Biscay in the summer period always held a fascination for Martin and he wrote an article detailing the 'Spanish Plume', a particular event which brings prolonged rain to parts of Britain. He wrote in connection with the October 1987 storm, an event which absorbed a good deal of his time for months afterwards. His latest passion was the concept of probability forecasting and in an effort to make forecasters more aware of the ideas and value of such forecasts he published a paper in the *Meteorological Magazine.*

After the Meteorological Office became an Agency he moved from Assistant Director of CFO to a new post in Product Development in which he was able to develop new products for the rapidly expanding commercial market. It was during this period that ill health began to dog him despite his healthy lifestyle. He invariably cycled in from Crowthorne (some five miles) each day in his rather striking purple shorts, he played squash, and felt something was missing if he didn't have his daily swim. Indeed he loved sport generally, especially cricket, and he rarely missed a rugby match that was on the television. It was during a swim while in Vancouver for a conference in the Autumn of 1992 that his health took a serious turn for the worse. He managed with great difficulty to deliver his presentation the following day but then returned home and into hospital. With great determination he fought his illness and was even able to visit the Office in late November, but in the end recovery was not to be. Many of his friends and colleagues took part at a Service of Thanksgiving for his life prior to his cremation on 12 January 1993. He is survived by his wife, Barbara, two sons and a daughter.

GUIDE TO AUTHORS

Content

Articles on all aspects of meteorology are welcomed, particularly those which describe results of research in applied meteorology or the development of practical forecasting techniques.

Preparation and submission of articles

Articles, which must be in English, should be typed, double-spaced with wide margins, on one side only of A4-size paper. Tables, references and figure captions should be typed separately. Spelling should conform to the preferred spelling in the *Concise Oxford Dictionary* (latest edition). Articles prepared on floppy disk (IBM-compatible or Apple Macintosh) can be labour-saving, but only a print-out should be submitted in the first instance.

References should be made using the Harvard system (author/date) and full details should be given at the end of the text. If a document is unpublished, details must be given of the library where it may be seen. Documents which are not available to enquirers must not be referred to, except by 'personal communication'.

Tables should be numbered consecutively using roman numerals and provided with headings.

Mathematical notation should be written with extreme care. Particular care should be taken to differentiate between Greek letters and Roman letters for which they could be mistaken. Double subscripts and superscripts should be avoided, as they are difficult to typeset and read. Notation should be kept as simple as possible. Guidance is given in BS1991: Part 1:1976 and *Quantities, Units and Symbols* published by the Royal Society. SI units, or units approved by the World Meteorological Organization, should be used.

Articles for publication and all other communications for the Editor should be addressed to: The Editor, Meteorological Magazine, Meteorological Office Room 709, London Road, Bracknell, Berkshire RG12 2SZ.

Illustrations

Diagrams must be drawn clearly, preferably in ink, and should not contain any unnecessary or irrelevant details Explanatory text should not appear on the diagram itself but in the caption. Captions should be typed on a separate sheet of paper and should, as far as possible, explain the meanings of the diagrams without the reader having to refer to the text. The sequential numbering should correspond with the sequential referrals in the text.

Sharp monochrome photographs on glossy paper are preferred; colour prints are acceptable but the use of colour is at the Editor's discretion.

Copyright

Authors should identify the holder of the copyright for their work when they first submit contributions.

Free copies

Three free copies of the magazine (one for a book review) are provided for authors of articles published in it. Separate offprints for each article are not provided.

Contributions: It is requested that all communications to the Editor and books for review be addressed to The Editor, Meteorological Magazine, Meteorological Office Room 709, London Road, Bracknell, Berkshire RG12 2SZ. Contributors are asked to comply with the guidelines given in the Guide to authors (above). The responsibility for facts and opinions expressed in the signed articles and letters published in *Meteorological Magazine* rests with their respective authors.

Subscriptions: Annual subscription £38.00 including postage; individual copies £3.40 including postage. Applications for postal subscriptions should be made to HMSO, PO Box 276, London SW8 SDT; subscription enquiries 071-873 8499.

Back numbers: Full-size reprints of Vols 1–75 (1866–1940) are available from Johnson Reprint Co. Ltd., 24–28 Oval Road, London NW1 7DX. Complete volumes of *Meteorological Magazine* commencing with volume 54 are available on microfilm from University Microfilms International, 18 Bedford Row, London WC1R 4EJ. Information on microfiche issues is available from Kraus Microfiche, Rte 100, Milwood, NY 10546, USA.

May 1993

Edited by R.M. Blackall
Editorial Board: R.J. Allam, N. Wood, W.H. Moores, J. Gloster, C. Nicholass, G. Lupton, F.R. Hayes

Vol. 122
No. 1450

Contents

ISSN 0026—1 149

Printed in the UK for HMSO, Dd 291241, 7/93, C12, 543, 24530